

**STREAMING BIREFRINGENCE STUDY OF THE  
INTERACTIONS OF SUBMICROSCOPIC PARTICLES**

**Thesis by  
Marcos Intaglietta**

**In Partial Fulfillment of the Requirements  
For the Degree of  
Doctor of Philosophy**

**California Institute of Technology  
Pasadena, California**

**1963**

## ACKNOWLEDGMENTS

The author wishes to thank Professor J. Harold Wayland for suggesting the research, directing it, and offering much helpful advice and encouragement.

Thanks are also due to Professor D. A. Morelli for helping in the design of the polarimeter, and to Dr. J. Vinograd for having conducted the ultracentrifuge tests and for having helped with many discussions.

The author wishes to thank Dr. N. S. Simmons of the Department and Laboratories of Nuclear Medicine and Radiation Biology of the University of California Medical Center at Los Angeles for having provided the samples of tobacco mosaic virus. He is also indebted to Professor E. W. Merrill of the School of Chemical Engineering of the Massachusetts Institute of Technology for making it possible to conduct the necessary viscosity measurements at his laboratory.

Thanks are due to the Applied Physics Corporation of Monrovia for having loaned the electronic equipment. Appreciation is expressed to Mr. P. V. Knust-Graichen for having isolated the southern bean mosaic virus and for having helped conduct the experiments, and to Mrs. Roberta Duffy for typing the manuscript.

This investigation was supported by a grant from the National Institutes of Health of the United States Public Health Service.

## ABSTRACT

An apparatus for the observation of streaming birefringence with photoelectric detection, in which the output signal near the null is linear with respect to the angular distance to the null, was built and tested. It was found that such an apparatus is able to establish the position of the isocline with an accuracy of one degree for a relative retardation of  $10^{-9}$ .

The apparatus was subsequently used to study the streaming birefringence of tobacco mosaic virus and of mixtures of tobacco mosaic virus and southern bean mosaic virus. Accurate measurements of the angle of isocline of both types of solutions showed that no significant difference exists between the experimental and theoretical results, once all the sources of extraneous birefringences are accounted for.

The amount of retardation of the mixtures was found to be lower than that for pure tobacco mosaic virus at equal concentrations of the latter and equal velocity gradients. This experimental result is explained by considering that the random motion of the spherical particles interacts with the orderly rotation of the rod-like particles, decreasing the amount of aligned material, and thus the amount of retardation.

## TABLE OF CONTENTS

PART	TITLE	PAGE
	Acknowledgment	
	Abstract	
	Table of Contents	
I.	INTRODUCTION	1
II.	THEORY OF MEASUREMENT OF STREAMING BIREFRINGENCE	7
	2.1 Optical System	7
	2.2 Separation of Extraneous Effects	18
III.	EXPERIMENTAL TECHNIQUE	24
	3.1 Equipment	24
	3.2 Alignment	29
	3.3 Data Handling	31
IV.	EXPERIMENTAL RESULTS	36
V.	DISCUSSION OF EXPERIMENTAL RESULTS AND CONCLUSIONS	51
	APPENDIX A - Theoretical Derivation of the SBR of a Solution of Long Slender Rods	63
	A.1 Motion of a Particle According to Hydrodynamic Theory	64
	A.2 Motion of the Particles Due to Brownian Motion and Rotary Diffusion	78
	A.3 Distribution Function	79
	A.4 Optical Behavior	81
	APPENDIX B - Sample Data	90
	References	94

## I. INTRODUCTION

The path of a beam of light in a transparent medium can be described through the use of Huygen's principle, which states that each element of a wave front may be regarded as the center of a secondary disturbance which gives rise to wavelets. These wavelets propagate with a velocity equal to the velocity of propagation of the wave. The position of the wave front at any later time is given by the envelope of all wavelets.

In the general case of an anisotropic medium, two sets of Huygen's wavelets propagate from every wave front. Substances having this property are said to exhibit birefringence. When there is a direction along which the velocity of propagation of the two sets of wavelets is equal, the substance is said to be uniaxial, and this direction is called the optic axis. In an uniaxial crystal there are two indices of refraction which characterize the two sets of Huygen's wavelets, with maximum and minimum values in directions perpendicular to each other and to the optic axis. One set of wavelets is spherical and its velocity of propagation is characterized by an index of refraction  $n_o$ . The second set is ellipsoidal and has a maximum index of refraction  $n_e$  in a direction perpendicular to the optic axis. The amount of birefringence is defined as the difference  $(n_o - n_e)$  between the two indices.

Birefringence can be produced in liquids by the influence of electric and magnetic fields, the presence of sound waves, and the existence of velocity gradients. This last effect constitutes streaming birefringence (SBR), and occurs in certain pure liquids as well as in solutions containing asymmetrical molecules.

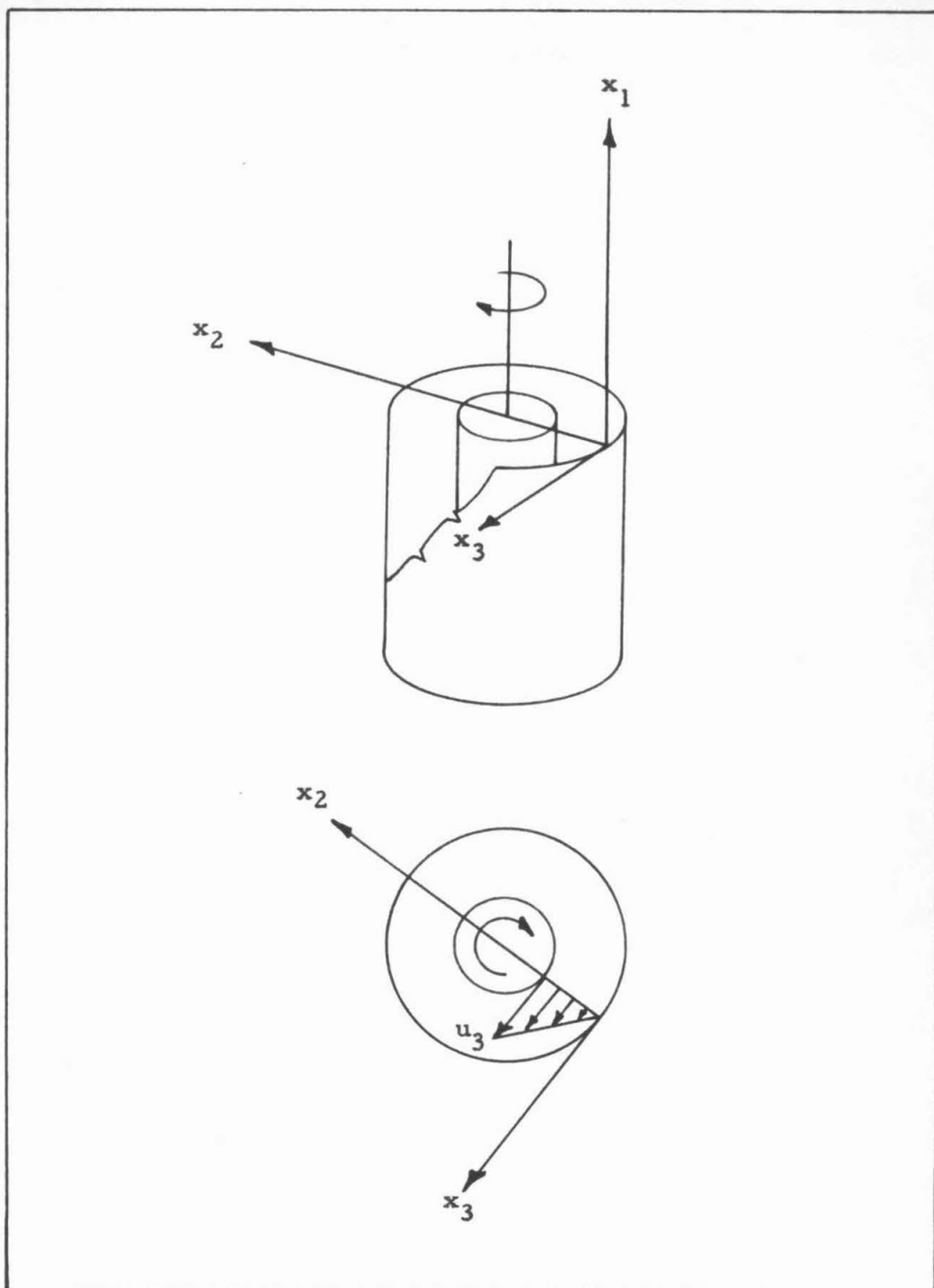


Figure 1. Location of the coordinate system with respect to surfaces in experimental apparatus. The phenomena are observed along the  $x_1$  direction. The solution is contained between the two concentric cylinders.

SBR is usually studied in solutions contained in the gap between two concentric cylinders, such that the rotation of either will cause a very nearly linear velocity gradient in laminar flow, characterized by:

$$u_3 = G x_2$$

which makes the solution become birefringent, with the amount of birefringence increasing steadily with the velocity gradient  $G$ . In this flow configuration (Figure 1), a given volume element will have the directions of maximum and minimum indices of refraction in the  $x_2x_3$  plane, where the smallest angle between the axis with the largest index of refraction and the streamline is the angle of isocline  $\chi$ . The amount of birefringence  $\Delta n$  for a given wavelength  $\lambda$  is obtained from the relation:

$$\Delta n = (n_o - n_e) = \frac{\lambda \delta}{2\pi l} = f(G)$$

where  $\delta$  is the observed phase difference between the two directions in radians, and  $l$  is the length of the path through the streaming fluid. At small gradients in laminar flow,  $\chi$  has been observed to approach  $45^\circ$  and  $\Delta n$  is proportional to  $G$ . At higher gradients  $\chi$  decreases, while  $\Delta n$  increases deviating from proportionality with  $G$ .

The behavior of solutions of small, rigid, asymmetric particles is explained by analyzing the motion of a single particle. In the presence of a linear velocity gradient in laminar flow, the particle is compelled to rotate with a non-uniform angular velocity, which makes it remain a longer time in the direction with smaller angular velocity. Brownian motion tends to counteract this hydrodynamic orientation, so that the competition of both influences establishes the probability that a

particle might have a certain angular position. The coupling of the angular distribution with the optical anisotropy of a particle yields the two main optical directions in the fluid as the directions of larger and smaller angular density.

The phenomenon was first observed by Maxwell<sup>(1)</sup> in 1866, and reported in 1873 in a paper which also described a concentric cylinder apparatus in which SBR could easily be produced.

Several theories have been proposed to explain the experimental evidence, the most successful at present being that of Peterlin and Stuart<sup>(2)</sup>. This theory assumes that a system of rigid, submicroscopic particles of ellipsoidal shape suspended in a medium becomes optically anisotropic when it is subjected to shear, due to the non-uniform motion of the particles. The theory has been extended to non-rigid particles, to the presence of heterogeneous populations, and to the superimposition of magnetic and electric fields.

The techniques of SBR were found to be applicable to the study of flow patterns in two-dimensional flow fields, and to the characterization of macromolecules. In the latter field, useful information from submicroscopic particles in solution can be obtained by relating the size, shape, mass, and dispersity of the particles to the optical properties of the system. Particularly significant is the data that can be obtained by extrapolation to zero shear, a method by which the rotary diffusion constant can be determined, as well as giving one indication as to the existence of a certain degree of structurization in the liquid.

In view of the above considerations, it has been the aim of experimenters to refine the measuring techniques so that the extremely

small effects characteristic of small concentrations and shears could be analyzed and interpreted. In successive refinements of the measuring techniques, some departures from the Peterlin and Stuart theory have been found, precisely in the range of small shears and concentrations, which is the most interesting in terms of characterization of macromolecules. Thus, it became apparent that there was need for an instrument whose sensitivity was significantly greater than anything previously used, in order to determine what these departures are.

The amount of SBR, and the location of the angle of isocline, is usually converted into an optical rotation for small birefringences by means of a quarter-wave plate, so that the location of the angles of interest is found by noting the position at which an analyzing prism extinguishes the light transmitted through the system. Originally, the null was observed directly by eye. In following refinements, the eye was replaced by a photomultiplier. This substitution was not always satisfactory, in that the increase in sensitivity was frequently offset by an increase in the noise that the photomultiplier picked up. Furthermore, simply substituting the photomultiplier for the eye did not eliminate the inherent characteristic of the signal to be detected, which depends on the square of the angle  $\epsilon$  between the position of the analyzer and the null.

Wayland<sup>(3)</sup> proposed to eliminate these difficulties by modulating sinusoidally the beam of light, by periodically rotating the plane of polarization of the light beam through a small angle  $\gamma_0$ , so that the sinusoidal signal transmitted by the analyzing prism had an amplitude varying linearly with the angle  $\epsilon$ . This system was found to have an

inherently larger signal to noise ratio than other systems, and since the output signal could be synchronously rectified so that in traversing the null the signal changed polarity, a very clear indication of the null was obtained.

In what follows, an apparatus built according to Wayland's principle is described; its performance is analyzed in terms of measurements of SBR made of solutions of tobacco mosaic virus (TMV), and mixtures of southern bean mosaic virus (SBMV) and TMV; and the basic theory of SBR is outlined.

## II. THEORY OF MEASUREMENT OF STREAMING BIREFRINGENCE

### 2.1 Optical System.

The net effect of the optical anisotropy produced in the flowing solution is described in Peterlin and Stuart (loc. cit.) by the following equations (see Appendix for their derivation):

$$\chi\left(\frac{G}{D}, p\right) = \frac{\pi}{4} - \frac{1}{12} \frac{G}{D} + \frac{1}{1296} \left(\frac{G}{D}\right)^3 + \dots$$

$$\Delta n = \frac{2\pi p}{15 \rho_p n D_p} (g_{x_1}' - g_{x_2}') c G \eta_m$$

where  $D$  is the rotational diffusion constant,  $D_p$  is the rotational diffusion constant with the viscosity that the particle experiences  $\eta_p$  divided out,  $p$  is a parameter characteristic of the axial ratio,  $n$  is the index of refraction of the medium,  $(g_{x_1}' - g_{x_2}')$  an optical factor characteristic of the particle and medium, and  $c$  is the concentration. This optical anisotropy converts linearly polarized light passing through a solution into elliptically polarized light. From the orientation of the characteristic ellipses the location of the two main directions in the medium is obtained, and from the degree of ellipticity the relative retardation is deduced, and thus the difference in indices of refraction.

The state of polarization of a beam of light can be described by a column matrix  $\{L\}$  whose elements  $I, Q, U, V$ , constitute Stokes' parameters. These are given by the following relations:

$$\begin{aligned} I &= (E_2^2 + E_3^2) & U &= (2E_2E_3 \cos\delta) \\ Q &= (E_2^2 - E_3^2) & V &= (2E_2E_3 \sin\delta) \end{aligned} \tag{1}$$

where  $E_2$  and  $E_3$  are instantaneous positive definite values of the components of the electric field in the  $x_2x_3$  plane of the system of coordinates shown in Figure 1, and the brackets, in this case, represent time averages.  $I$  is a measure of the intensity of the beam of light;  $Q, U, V$  are measures of the state of polarization. The beam of light propagates along the  $x_1$  direction.  $\delta$  is the instantaneous phase difference between the two directions; and a beam of unpolarized light, intensity-normalized, is described by:

$$\{L\} = \{1, 0, 0, 0\} .$$

For an elliptically polarized beam of light, the ratio  $E_2/E_3$  and the angle  $\delta$  are constant. With reference to Figure 2, the components  $I, Q, U, V$  are shown by Born<sup>(4)</sup> to be:

$$\begin{aligned} I &= 1 & U &= \cos 2\alpha \sin 2\chi \\ Q &= \cos 2\alpha \cos 2\chi & V &= \sin 2\alpha \end{aligned} \quad (2)$$

where  $\tan 2\alpha = E_2/E_3 = (n_2/n_3)^2$ , and the intensity is normalized.

The action of an optical device is to transform the polarization of a beam of light from one state to another, and since both states can be represented by a 4-vector, a  $4 \times 4$  matrix will adequately represent such a transformation. These matrices are found empirically and are listed by Walker<sup>(5)</sup> and Shurcliff<sup>(6)</sup>. A series of optical devices is then represented by the product of their individual matrices.

The birefringent solution is represented by the matrix

$[M(\beta, \delta)] :$

$$[M(\beta, \delta)] = \begin{bmatrix} 1 & 0 & 0 & 0 \\ 0 & \cos^2 2\beta + \sin^2 2\beta \cos \delta & \cos 2\beta \sin 2\beta (1 - \cos \delta) \sin 2\beta \sin \delta \\ 0 & \sin 2\beta \cos 2\beta (1 - \cos \delta) & \sin^2 2\beta + \cos^2 2\beta \cos \delta - \cos 2\beta \sin \delta \\ 0 & -\sin 2\beta \sin \delta & \cos 2\beta \sin \delta & \cos \delta \end{bmatrix} \quad (3)$$

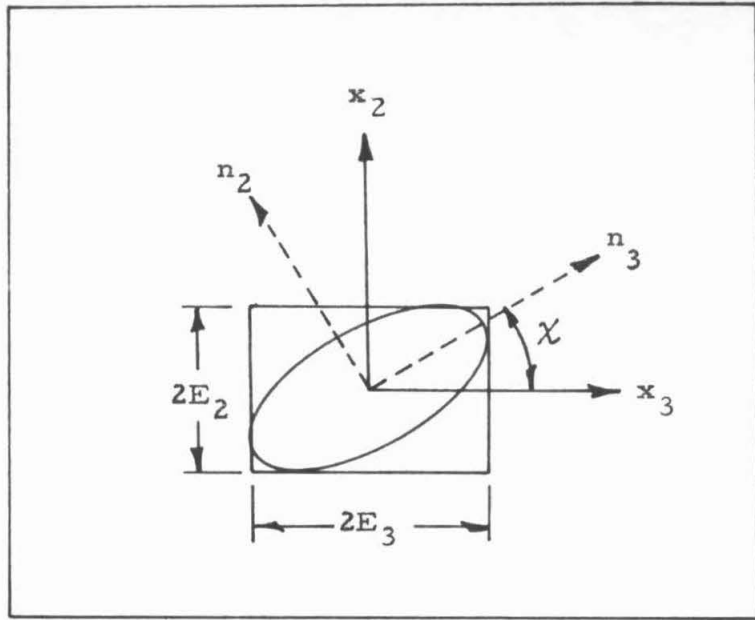


Figure 2. Ellipse resulting from the superposition at right angles of two simple harmonic motions of amplitudes  $E_2$  and  $E_3$  having the same frequency but difference phase.

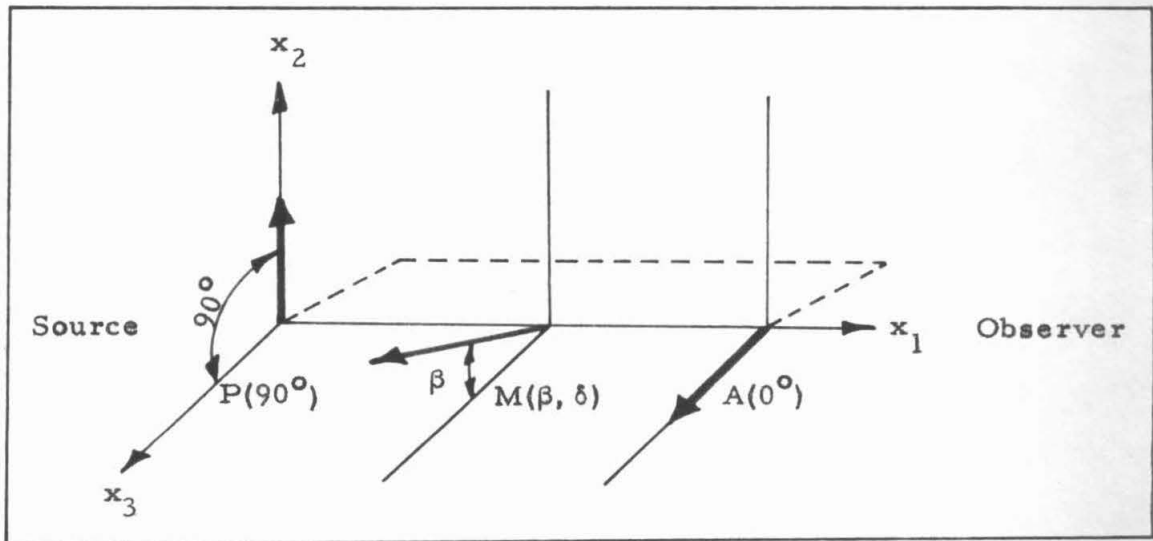


Figure 3. Diagrammatic scheme of a simple optical system for the analysis of a birefringent medium. The polarizer and analyzer are made to rotate together about the optic axis, for the determination of  $\beta$ .

where  $\beta$  is the orientation of the direction in the medium that possesses the largest index of refraction, and  $\delta$  is the phase difference that the medium will induce between components polarized in the two main directions, when the beam of light traverses it along the optic axis.

The simplest technique for analyzing a birefringent medium is to observe the effect that it has on a beam of plane polarized light that traverses it. A beam of polarized light is obtained by having a beam of light first go through a total polarizer  $[P(90^\circ)]$ , such as a Glan-Thompson prism. This beam is first made to traverse the birefringent medium and is observed through another polarizer  $[A(0^\circ)]$  locked in quadrature with the first polarizer, as shown diagrammatically in Figure 3.

With the optic axis along the  $x_1$  coordinate, and the two total polarizers oriented as shown in Figure 3, the matrices that characterize them are:

$$[P(90^\circ)] = \frac{1}{2} \begin{bmatrix} 1 & -1 & 0 & 0 \\ -1 & 1 & 0 & 0 \\ 0 & 0 & 0 & 0 \\ 0 & 0 & 0 & 0 \end{bmatrix}; [A(0^\circ)] = \frac{1}{2} \begin{bmatrix} 1 & 1 & 0 & 0 \\ 1 & 1 & 0 & 0 \\ 0 & 0 & 0 & 0 \\ 0 & 0 & 0 & 0 \end{bmatrix}$$

The normalized transmission of this system is given by the intensity component  $I$  of the  $\{L_o\}$  vector which results from the equation:

$$\{L_o\} = [A(0^\circ)][M(\beta, \delta)][P(90^\circ)]\{L_i\}. \quad (4)$$

where the matrices transform the incident beam of light  $\{L_i\}$  in the same order as the beam encounters the optical elements. Substituting the corresponding matrices into equation (4) and evaluating the term corresponding to the intensity of the transmitted beam, one obtains:

$$I = \frac{1}{4} [1 - (\cos^2 2\beta + \sin^2 2\beta \cos \delta)]$$

which, for small  $\beta$  and  $\delta$ , reduces to:

$$I \cong \frac{1}{2} \beta^2 \delta^2. \quad (5)$$

Clearly then, rotating the polarizer-analyzer assembly with respect to the birefringent medium  $[M(\beta, \delta)]$  through an angle  $\beta$  will result in the complete extinction of the transmitted light, and the position of the optical axis of the polarizing prism will then coincide with the optical axis of the birefringent medium. From this analysis it becomes apparent that due to the quadratic dependence of the intensity of the transmitted light to the angular difference between analyzer axis and medium axis  $\beta$ , the definition of the null is quite poor.

To determine the ellipticity of the polarization in the beam of light, a quarter-wave retarder is inserted after the birefringent medium. The fast axis of this element is located parallel to the axis of the analyzer, such that the matrix  $[Q(0^\circ, \frac{\pi}{2})]$  of this element is given by:

$$[Q(0^\circ, \frac{\pi}{2})] = \begin{bmatrix} 1 & 0 & 0 & 0 \\ 0 & 1 & 0 & 0 \\ 0 & 0 & 0 & -1 \\ 0 & 0 & 1 & 0 \end{bmatrix}$$

and the optical system can be represented diagrammatically as in Figure 4, where the polarizer and quarter-wave plate are now locked together. The birefringent medium is then rotated so that its optical axis makes an angle of  $45^\circ$  with the axis of the polarizer. The intensity of the beam of light emerging from this system is obtained from the following equation:

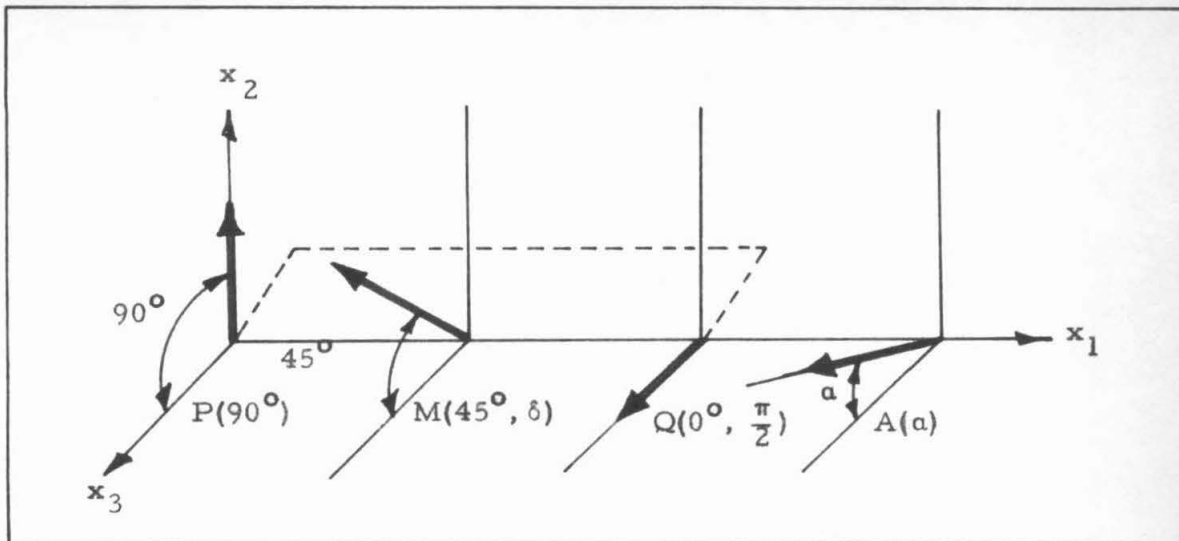


Figure 4. Diagrammatic scheme of the determination of the amount of retardation  $\delta$ .

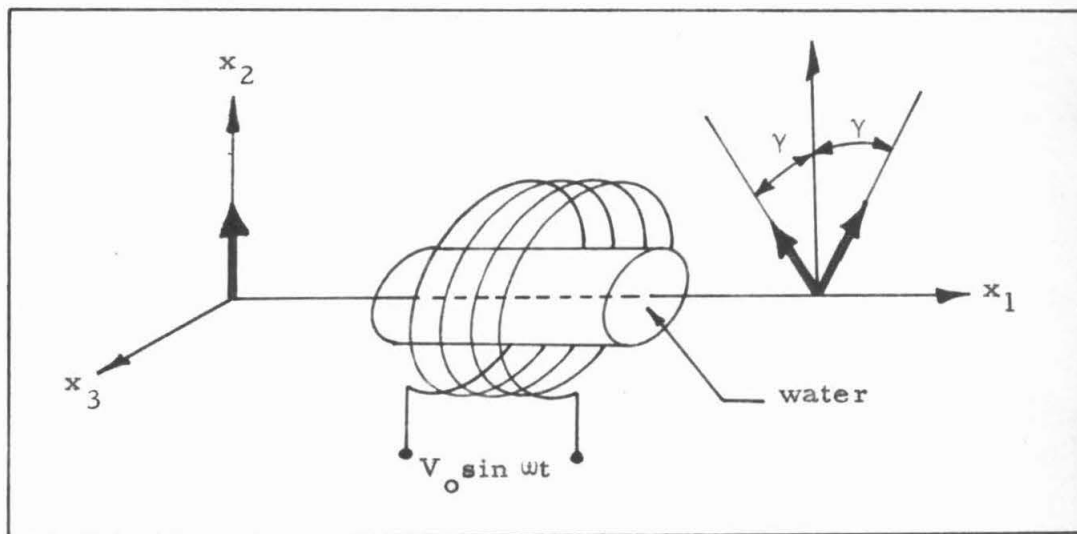


Figure 5. Diagrammatic scheme of the Faraday effect. Applying a sinusoidal voltage to the winding, a magnetic field along the  $x_1$  axis is produced that changes in direction with frequency  $\omega$ . A beam polarized along the  $x_2$  axis will be rotated through an angle  $\gamma = \gamma_0 \sin \omega t$ , the sign of the rotation being determined by the instantaneous direction of the field.

$$\{L_0\} = [A(\alpha)][Q(0^\circ, \frac{\pi}{2})][M(45^\circ, \delta)][P(90^\circ)][L_1] \quad (6)$$

where:

$$[A(\alpha)] = \frac{1}{2} \begin{bmatrix} 1 & \cos 2\alpha & \sin 2\alpha & 0 \\ \cos 2\alpha & \cos^2 2\alpha & \sin 2\alpha \cos 2\alpha & 0 \\ \sin 2\alpha & \sin 2\alpha \cos 2\alpha & \sin^2 2\alpha & 0 \\ 0 & 0 & 0 & 0 \end{bmatrix} \quad (7)$$

$[A(\alpha)]$  being the matrix of a polarizer oriented with its axis along the  $\alpha$  direction.

The transmitted light is:

$$I = \frac{1}{4} [1 - \cos (2\alpha - \delta)];$$

thus locating the analyzer at an angle  $\alpha = \frac{1}{2}\delta$  extinction is obtained and the retardation is determined. For a small angular distance  $\epsilon$  from the location of this null, assuming that there is no error in the location of the angle of isocline, and for small retardations  $\delta$ , the transmission of this system is given by the following expression:

$$I \cong \epsilon^2/2.$$

It is thus apparent that the intensity of the transmitted light in the vicinity of the null, and for small retardations, is not linear with the error angle, which results in a poor definition of this null.

A system for which the approach to the null is linear in the error angle can be conceptually realized because the matrix (3) contains elements that are linear in both  $\beta$  and  $\delta$  simultaneously. Thus, a device must be found so that those linear elements are the ones that characterize the angular dependence of the intensity in the proximity of the null. Wayland (loc. cit.) proposed to use a Faraday effect

modulator (FEM) to bring about the necessary shift in the elements of matrix (3), and Wayland and Badoz<sup>(7)</sup> proposed a system in which the quarter-wave plate was permanently in place, oriented with its axis parallel to the axis of the analyzer.

The Faraday effect consists in a rotation that a beam of polarized light experiences in traversing a medium in which there is a magnetic field parallel to the direction of the beam of light. This effect is exhibited by a variety of substances in the solid, liquid, and gaseous state, and is characterized by Verdet's constant, which for a given substance relates the amount of optical rotation at a given wave length to the magnetic field strength that causes it, and the thickness of material traversed by the beam of light. Among the most convenient substances that exhibit this effect is water, which has a relatively large rotation, and being a liquid does not introduce extraneous birefringence in the system other than for the windows that contain it in place. The Faraday cell is shown schematically in Figure 5. The effect can be produced both by a steady magnetic field, which produces a simple rotation, or by a field that is alternating in direction, as the one produced by an AC solenoid which produces an alternating rotation at the driving frequency. The latter property is particularly significant in this development since the net result of this alternating rotation is to produce a modulated signal suitable for electronic amplification.

An optical device that rotates the plane of polarization of a beam of light by an angle  $\gamma$  is characterized by the matrix:

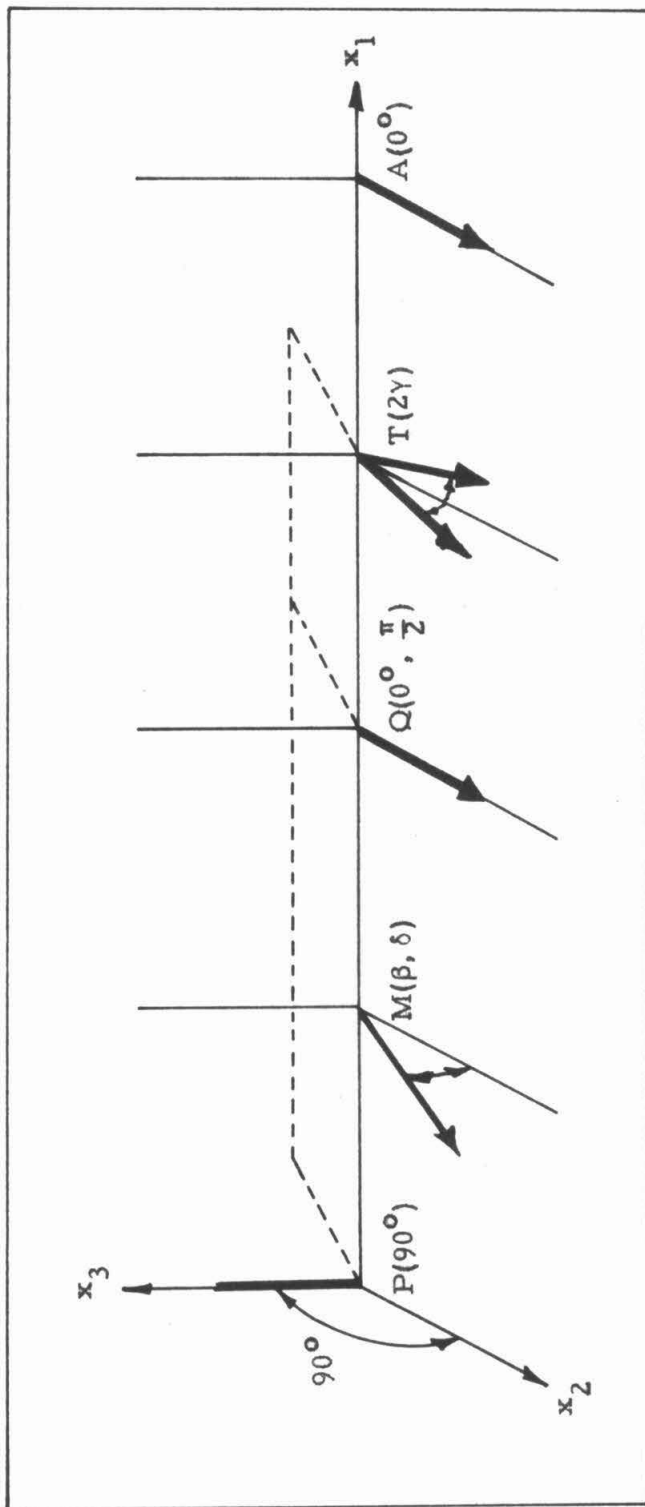


Figure 6. Diagrammatic scheme of polarimeter incorporating a Faraday effect modulator,  $T(2\gamma)$ .

$$[T(2\gamma)] = \begin{bmatrix} 1 & 0 & 0 & 0 \\ 0 & \cos 2\gamma & \sin 2\gamma & 0 \\ 0 & -\sin 2\gamma & \cos 2\gamma & 0 \\ 0 & 0 & 0 & 1 \end{bmatrix}$$

which, when located as shown diagrammatically in Figure 6, operates on a beam of light by premultiplying the whole matrix product up to  $[A(0^\circ)]$  by the matrix  $[T(-2\gamma)]$  and postmultiplying the same quantity by the matrix  $[T(2\gamma)]$ . In this case, since the solenoid is driven by an AC source,  $\gamma = \gamma_0 \sin \omega t$ . The intensity of the transmitted light of the system of Figure 6 is obtained by evaluating the intensity component of the emerging beam of light  $\{L_0\}$  in the following equation:

$$\{L_0\} = [A(0^\circ)][T(-2\gamma)][Q(0^\circ, \frac{\pi}{2})][M(\beta, \delta)][P(90^\circ)][T(2\gamma)]\{L_1\}. \quad (8)$$

The intensity of the transmitted light is given by:

$$I = \frac{1}{4} [1 - \cos 2\gamma (\cos^2 2\beta + \sin^2 2\beta \cos \delta) - \sin 2\gamma \sin 2\beta \sin \delta]. \quad (9)$$

For small angles  $\gamma$  the terms in  $\cos 2\gamma$  and  $\sin 2\gamma$  can be expanded into a series. Carrying out this expansion, it can be seen that the only term that oscillates at the driving frequency is the first term of the sine expansion, while the cosine expansion yields a DC term and terms that are a function of integral multiples of the doubled frequency.

Therefore, an amplifier tuned to the fundamental frequency with appropriate filtering for the higher harmonics will pick up a steady background noise resulting from the DC term, and a signal at the fundamental frequency given by the expression:

$$I = \frac{1}{4} \sin 2\gamma \sin 2\beta \sin \delta \approx \delta \beta \gamma_0 \sin \omega t \quad (10)$$

which is linear in both  $\delta$  and  $\beta$  for small angles. To locate the

angle of isocline, the whole system shown in Figure 6 is rotated until extinction is achieved. The orientation of the polarizer corresponds then to the orientation of the isocline in the medium.

To determine the amount of birefringence, as in the previous case, the whole assembly of polarizer, quarter-wave plate, and analyzer is rotated through  $45^\circ$  from the position  $\beta$  of the axis of the medium. Since phenomenologically it is equivalent to rotate the birefringent medium through  $45^\circ$  keeping the optical assembly fixed, in the following equations the medium is rotated in order to simplify the analysis.

The intensity of the transmitted light is again obtained by calculating the intensity component of the emerging beam of light  $\{L_o\}$  from the equation:

$$\{L_o\} = [A(\alpha)][T(-2\gamma)][Q(0^\circ, \frac{\pi}{2})][M(45^\circ, \delta)][P(90^\circ)][T(2\gamma)]\{L_i\} \quad (11)$$

which yields the result

$$I = \frac{1}{4} [1 - \cos 2\alpha (\cos 2\gamma \cos \delta - \sin 2\gamma \sin \delta) - \sin 2\alpha (\sin 2\gamma \cos \delta + \cos 2\gamma \sin \delta)]$$

from where it can be seen that a rotation of the analyzer of  $\alpha = \frac{1}{2}\delta$  produces a null that identifies the amount of birefringence  $\delta$ .

At a small angular distance  $\epsilon$  from the null, the transmitted intensity is given by the relation

$$I \cong \frac{1}{4} (1 - \cos 2\gamma - \epsilon \sin 2\gamma) \cong -\frac{1}{2} \epsilon \gamma$$

clearly linear in  $\epsilon$  for small angles.

It should be noted that in this system the quarter-wave plate is kept permanently in place, both for the determination of the angle of isocline and of the amount of birefringence. This feature is quite advantageous from the mechanical point of view, and does not appear in

the simple system.

## 2.2 Separation of Extraneous Effects.

The optical system considered so far assumes that both the light source and the optical elements are ideal in the sense that the source is a monochromatic point source, and that all windows are free of strain and thus of extraneous birefringence.

A monochromatic light source of satisfactory characteristics can be obtained from a high-pressure mercury arc discharge, from which a convenient spectral line is selected by means of an optical filter. Further details of this light source are given in the next section.

Regarding extraneous birefringences, the matter is more complex and requires careful analysis. In trying to detect the feeble signals characteristic of small concentrations and small shears, it has been found that with the photoelectric system under consideration the limiting factor is the relative size of the signals from the solution and the signals from the residual strains in the windows, which introduce birefringence.

Two sets of windows occur in the system. One contains the solution in place, in the annular gap between the concentric cylinders (Couette cell). The other contains the water in the FEM. Both sets introduce extraneous birefringences that are detectable with this system. Of the two, the one that is most easily accounted for is the one pertaining to the FEM windows.

To correct for the extraneous birefringence of the FEM windows, this device is mounted so that it constitutes one unit with the polarizer and quarter-wave plate. This mounting assures that the same angular

relationship between the axis of the polarizer and the extraneous birefringence of the FEM is maintained in the system.

The location of the angle of isocline presupposes that both polarizer and analyzer can be locked in quadrature, together with the quarter-wave plate. Clearly, if a birefringent medium is located between the two when this quadrature is established, a certain error will occur; therefore, it is important to establish how far from quadrature the polarizer and analyzer are when the null is established with the birefringence of the FEM windows in between.

The polarizer is assumed to be at  $90^\circ$  azimuth; the FEM windows are represented by the matrix  $[F(\beta_1, \delta_1)]$  which is of the same form as matrix (3), where their combined retardation is assumed to be  $\delta_1$ , with their isocline at  $\beta_1$ . The analyzer is then located at  $\alpha$ , which is assumed to be a small angle about zero azimuth. The transmission of this system is given as usual by the intensity component of the emerging beam of light  $\{L_0\}$  computed from the matrix equation:

$$\{L_0\} = [A(\alpha)][F(\beta_1, \delta_1)][P(90^\circ)]\{L_1\}. \quad (12)$$

After substituting the appropriate matrices into equation (12), the intensity component of the transmitted light is found to be:

$$I = 1 - \cos 2\alpha (\cos^2 2\beta_1 - \sin^2 2\beta_1 \cos \delta_1) - \sin 2\alpha \sin 2\beta_1 \cos 2\beta_1 (1 - \cos \delta_1) \quad (13)$$

For small  $\delta_1$ 's the following approximation is valid:

$$\cos \delta_1 \cong 1 - \frac{\delta_1^2}{2}$$

and equation (13) reduces to:

$$I = 1 - \cos 2\alpha \left(1 - \frac{\delta_1^2}{2} \sin^2 2\beta_1\right) - \frac{\delta_1^2}{2} \sin 2\alpha \sin 2\beta_1 \cos 2\beta_1,$$

which has a minimum at an angle  $\alpha$  such that

$$\tan 2\alpha \cong \frac{\delta_1^2 \sin 2\beta_1 \cos 2\beta_1}{2 - \delta_1^2 \sin^2 2\beta_1},$$

which for small  $\delta_1$ 's shows that the error angle  $\alpha$  by which the analyzer differs from quadrature is of the order  $(\delta_1^2)/2$  at most.

To see how this error in quadrature affects the location of the quarter-wave plate, this element is now installed in the system with its axis nearly in quadrature with the polarizer, i. e., at an angle  $\alpha_1$ , where  $\alpha_1$  is a small angle. The transmission of the system is now obtained as usual. Keeping in mind that the analyzer is located at an angle which is at most  $(\delta_1^2)/2$ , it can be approximated by the matrix:

$$[A(\frac{\delta^2}{2})] \cong \frac{1}{4} \begin{bmatrix} 2 & 2 & \delta^2 & 0 \\ 2 & 2 & \delta^2 & 0 \\ \delta^2 & \delta^2 & \frac{1}{2}\delta^4 & 0 \\ 0 & 0 & 0 & 0 \end{bmatrix}$$

The matrix of the quarter-wave plate at an angle  $\alpha_1$ , where  $\alpha_1$  is assumed small, is obtained directly from matrix (3) as

$$[Q(\alpha_1, \frac{\pi}{2})] \cong \begin{bmatrix} 1 & 0 & 0 & 0 \\ 0 & 1 & 2\alpha_1 & 2\alpha_1 \\ 0 & 2\alpha_1 & 4\alpha_1^2 & -1 \\ 0 & -2\alpha_1 & 1 & 0 \end{bmatrix}$$

Carrying out the usual computation for the intensity component of the transmitted light, it is found that

$$I \cong \frac{\delta^2}{2} \alpha_1,$$

which has a minimum at  $\alpha_1 = 0$ , which means that the quarter-wave

plate aligns in quadrature with the polarizer, and that extraneous birefringence of the FEM windows can be neglected for the usual amounts of residual birefringence found in these windows, which translates as a rotation of the order of  $10'$  of arc, as a maximum.

The most troublesome extraneous birefringence is the one belonging to the windows of the Couette cell. An important feature of the error that it produces is that the angular relationship between the axis of the polarizer and the one of the windows is not constant, since the nature of the measurements (location of the isocline,  $45^\circ$  shift) locates the axis of the polarizer at different places in a run. This then requires that the effect of the windows be known throughout the angular range of the instrument.

To establish the effect of the windows, a method was devised that determines simultaneously the retardation due to the windows, the axis of these, and the reference null for the quadrature of analyzer and polarizer. Furthermore, this method does not require the withdrawal of the Couette cell from the optical path every time that the reference null must be determined.

From equation (12) it can be seen that for every angular location of the polarizer, there is a different extinction angle  $\alpha_2$  of the analyzer. Assuming that the effect of the windows is small, i. e., small retardation  $\delta_w$ , the combined windows can be represented by the simplified form of matrix (3):

$$[M_w(\beta_w, \delta_w)] = \begin{bmatrix} 1 & 0 & 0 & 0 \\ 0 & 1 & 0 & \delta_w \sin 2\beta_w \\ 0 & 0 & 1 & -\delta_w \cos 2\beta_w \\ 0 & -\delta_w \sin 2\beta_w & \delta_w \cos 2\beta_w & 1 \end{bmatrix} \quad (14)$$

Substituting the above matrix into equation (12) and calculating the intensity of the transmitted light, it is found that for each polarizer setting  $\eta$  there is a minimum transmission for each analyzer setting  $\alpha_2$ , such that:

$$\tan 2\alpha_2 \cong \frac{-\delta_w \sin 2\eta}{1 + 2\gamma \delta_w \sin 2\eta}$$

which reduces to

$$\alpha_2 \cong \frac{1}{2} \delta_w \sin 2\eta \quad (15)$$

for small angles  $\delta_w$  and  $\gamma$ . Therefore, the minimum transmission angle of the analyzer describes a sine wave, whose amplitude is proportional to half the amount of retardation, and whose nodes represent the location of the axis of the windows, and can be used to establish the quadrature between the polarizer and analyzer.

The experimental data then consists of the measure of the isocline and amount of retardation of the composite system of windows and birefringent solution by the method outlined in the previous section, and the measure of the birefringence of the optical characteristics of the windows by the method of plotting the extinction angle as a function of the azimuth of the polarizer already outlined. It is now of considerable importance to establish whether the effect of the windows can be separated from the composite measurement to obtain the true birefringence of the flowing solution, particularly in those circumstances

where both effects are of the same order of magnitude.

For the small angles under consideration (less than one degree in either case), both the birefringent medium  $[M(\beta, \delta)]$  and the windows  $[M_w(\beta_w, \delta_w)]$  are approximated by the matrix (14). The net effect of the two media is equivalent to the product of the two matrices:

$$[M(\beta, \delta)][M_w(\beta_w, \delta_w)] \cong \begin{bmatrix} 1 & 0 & 0 & 0 \\ 0 & 1 & 0 & P_1 \\ 0 & 0 & 1 & -P_2 \\ 0 & -P_1 & P_2 & 1 \end{bmatrix} \quad (16)$$

where  $P_1 = \delta_w \sin 2\beta_w + \delta \sin 2\beta$  and  $P_2 = \delta_w \cos 2\beta_w + \delta \cos 2\beta$ , and products of the form  $\delta_w \delta$  have been neglected. Matrix (16) is of the same form as matrix (14). Setting the matrix  $[M_e(\beta_e, \delta_e)]$  to represent the experimental results, this last matrix can be equated term by term with matrix (14), and solving for  $\beta$  and  $\delta$  it is found that:

$$\delta^2 = \delta_e^2 + \delta_w^2 - 2\delta_e \delta_w \cos 2(\beta_e - \beta_w) \quad (17)$$

$$\tan 2\beta = \frac{\delta_e \sin 2\beta_e - \delta_w \sin 2\beta_w}{\delta_e \cos 2\beta_e - \delta_w \cos 2\beta_w} \quad (18)$$

### III. EXPERIMENTAL TECHNIQUE

#### 3.1 Equipment.

To take full advantage of the increase in sensitivity resulting from the combination of optical elements described in the previous section, a polarimeter head was designed and built. With reference to Figures 7, 8, and 9, the basic movement of the polarimeter (H) is the one of the transit head, where the concentricity of the axis of rotation is assured by the conical geometry of the bearing surfaces.

In accordance with the required movements, two concentric graduate circles (G) are mounted on the two independent sections of the system. The upper one, with a least count of  $0.01^\circ$ , records the position of the analyzing prism with respect to the lower one. The lower graduate circle, with a least count of  $1'$ , is integral with the polarizer (P), the quarter-wave plate (Q), and the FEM (F).

Both polarizing and analyzing prisms are calcite Glan-Thompson polarizers. The quarter-wave plate is a quartz crystal cut to such a thickness as to retard the  $5460 \text{ \AA}$  wavelength by one-quarter of this wavelength along its slow axis with respect to the fast one.

The Couette cell (C) is the same one used by Sutura<sup>(8)</sup> for the calibration of TMV solutions, with a modified mounting with metric adjustments for leveling its main axis.

The FEM (F) was built in such a way that an approximately uniform spherical sheet of current circulates about its axis. Such a geometry produces a uniform magnetic field parallel to the axis of revolution of the winding. A uniform magnetic field is required to produce a uniform effect throughout the complete cell, so that all the beam is

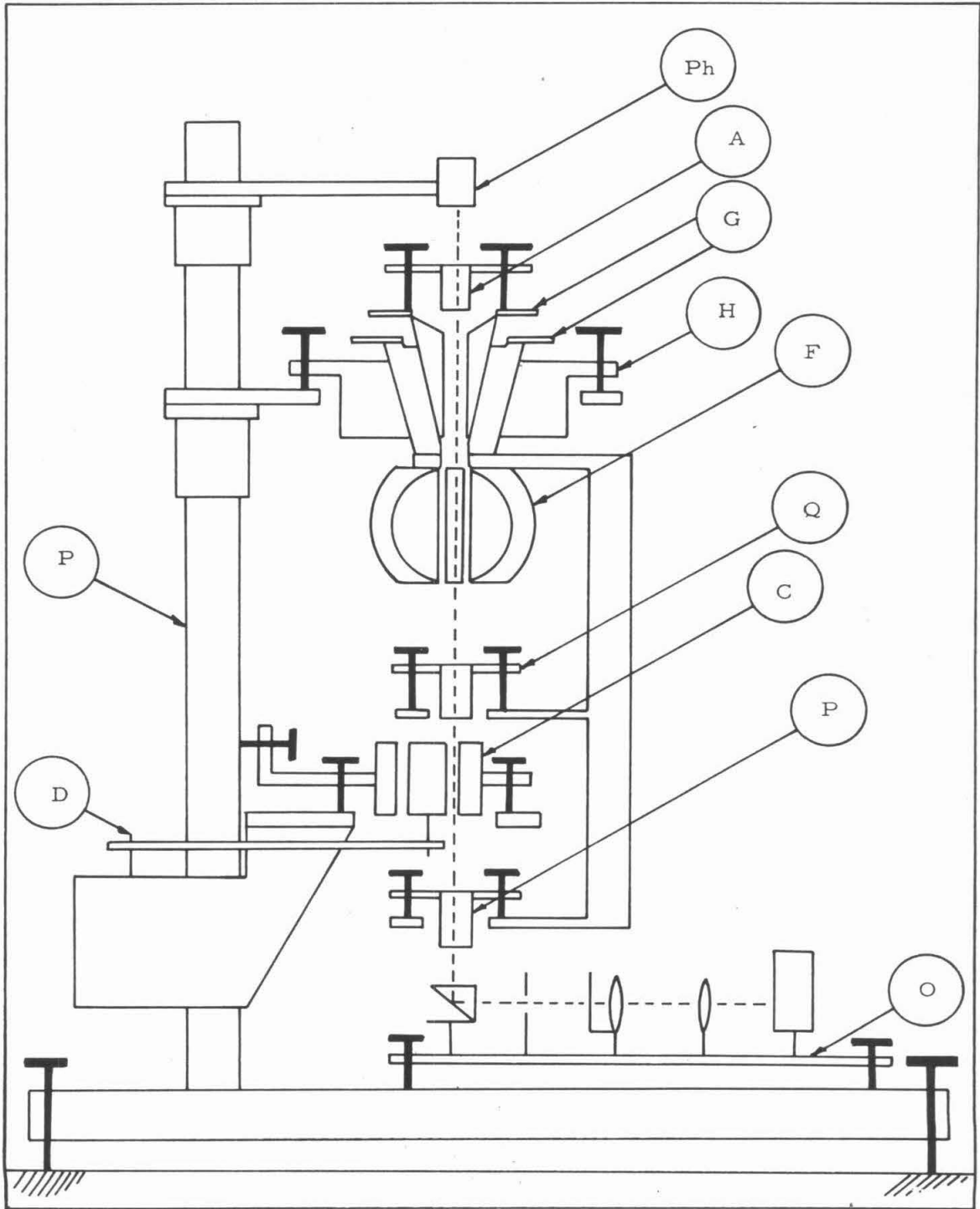


Figure 7. Diagram of apparatus. The dotted line represents the path of the beam of light.

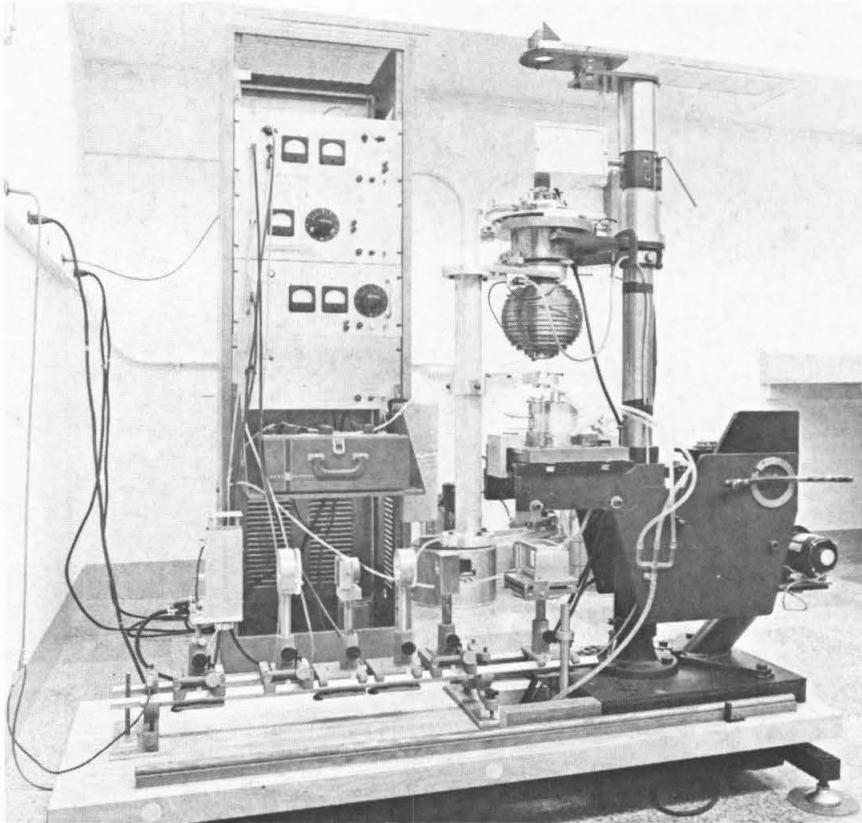


Figure 8. Overall view of apparatus.

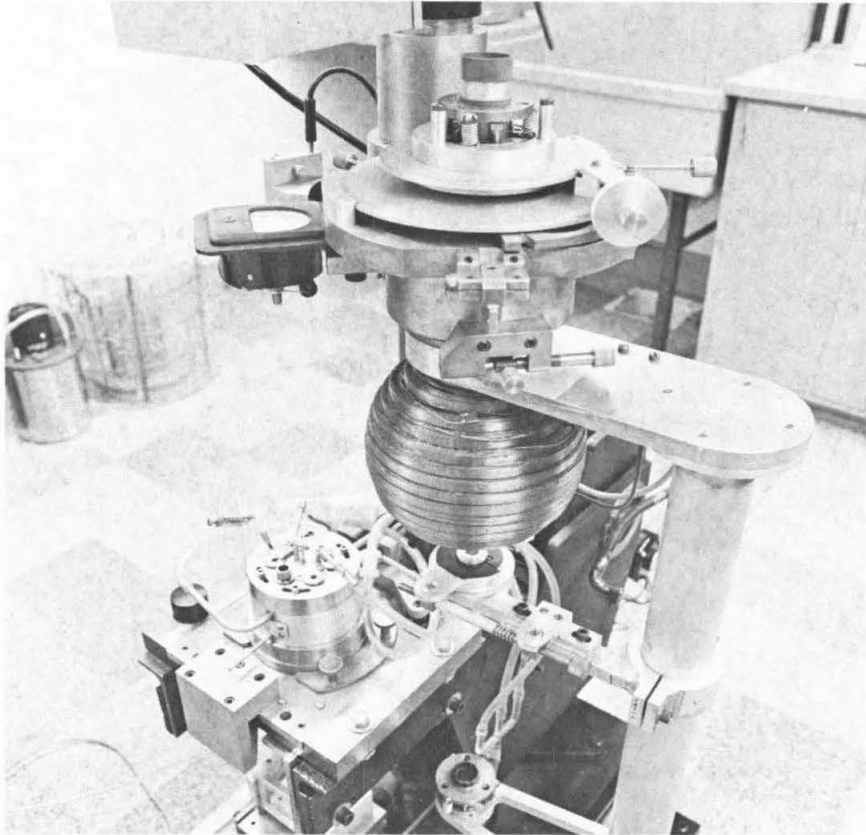


Figure 9. View of polarimeter.

uniformly retarded, and no errors result from placing the beam at different locations with respect to the axis of rotation. The water required is held in place by a lucite tube with strain-free optical windows. Special provision is made for trapping small air bubbles that develop in time.

The system can be rotated as a unit, or each part independently, including the quarter-wave plate. Micrometric adjustments exist for the three parts. A special indexing plate is also provided so that the system as a unit can be moved  $45^{\circ}$  from any attitude, which is required for the determination of the amount of birefringence. All optical elements are mounted so that they can further be micrometrically adjusted to perpendicularity to the optical axis of the system.

The complete polarimeter pivots about the post ( $P_0$ ) and can be swung out of the way of the Couette cell to facilitate its filling, which is usually complicated by small trapped bubbles. The drive (D) of the inner rotor consists of a synchronous motor, two pairs of interchangeable gears, and one interchangeable worm and gear reduction unit. Motion is transmitted to the cell through a timing belt that straddles the post.

The optical bench mounts a concentrated mercury arc lamp and a system of lenses that produce a narrow beam of light focused at the exit window of the filled Couette cell. The Couette cell uses a rotor which clears a 2 millimeter gap, while the cross section of the beam through the test section is 0.5 millimeters, to eliminate the possibility of reflections from the walls. A Wratten No. 77 optical filter selects the  $5460 \text{ \AA}$  line of the mercury discharge.

The FEM is driven by a variable transformer from the 120 volt, 60 cycle building supply at such a level as to produce about  $5^{\circ}$  modulation.

The photoelectric system, built by Applied Physics Corporation of Monrovia, consists of a photomultiplier, an amplifier whose gain is regulated by the amount of light that the photomultiplier receives and which is tuned to the 60-cycle frequency of the signal transmitted by the analyzing prism, and a synchronous switching rectifier driven by the same supply that drives the FEM.

The output of the amplifier gives a direct measure of the amount of unbalance between the location of the optical assembly and the optical axes of the system. Synchronous rectification is so arranged that the output signal changes phase in traversing the null, giving a very clear indication of the position of the null.

The mercury arc is an Osram 100W, and is driven by a DC power supply specially built for the purpose.

The whole laboratory is air conditioned and kept at  $20^{\circ}\text{C} \pm 1^{\circ}$ , and the Couette cell is thermostatted by circulating water kept at  $20^{\circ}\text{C} \pm 0.01$  by a Sargent temperature regulator that operates in thermal push-pull.

### 3.2 Alignment.

The system is first aligned along the direction of gravity by means of a precision level. The axes of the polarimeter and the Couette cell are aligned in such a manner. The axis of rotation of the polarimeter is made parallel to the direction of gravity by locating a level on either graduate circle and adjusting its orientation until no change in

the position of the bubble is detectable in any attitude of the system. The main axis of the Couette cell is aligned by withdrawing the cover and adjusting the cell until a level placed on it shows the same bubble position for all positions of the level.

The optical elements are first adjusted in the horizontal plane and their cylindrical mountings are made concentric with the axis of rotation of the system by means of a precision dial gauge.

Finally, the surfaces of the polarizing prisms and the quarter-wave plate are made perpendicular to the axis of rotation, by adjusting their tilt until the reflected image of the cross hairs of an autocollimator shows no relative movements as the whole assembly is rotated.

Once the optical system is aligned, a beam of light from the mercury discharge arc is so arranged that its circular cross sections at the entrance of the polarizer and the exit of the analyzer prisms are well clear of their edges. The beam is made to focus at the exit window of the filled Couette cell. A 0.5 millimeter diaphragm at the entrance window of the Couette cell is located in such a manner that the light going through it is centered in the 2 millimeter gap. Because of the relative size of the source to the entrance diaphragm, the cross section of the beam is uniform throughout the test section. For this adjustment the Couette cell is moved in its horizontal plane until the beam is centered in the gap.

In addition to the mechanical alignment, the system is aligned photoelectrically, in the sense that quadrature between the two prisms and alignment of the quarter-wave plate is made using the photoelectric system as a detector.

Once the faces of the two prisms are aligned to perpendicularity to the axis of rotation and the beam of light is made concentric with this axis, and before putting the Couette cell and the quarter-wave plate in place, the position of quadrature of the two prisms is noted at different attitudes of the system. If no correction must be made at any attitude, the two prisms are considered parallel. The same procedure is used with the quarter-wave plate, where this is located in the appropriate direction by rotating it until extinction is obtained when the two prisms are in quadrature. Finally, the Couette cell is put in place without windows, and the procedure is again repeated to make certain that reflections from the walls do not introduce spurious effects.

The final alignment is electronic, where the phase of the switching relay of the amplifier is so adjusted that it exactly rectifies the sine wave that constitutes the output of the amplifier.

### 3.3 Data Handling.

Preliminary experiments with solutions of Bentonite and TMV indicated that the system constructed was capable of a considerably greater accuracy than any instrument previously built, provided that the effects of extraneous birefringences introduced by the windows could be properly accounted for or eliminated.

Considerable attention was given to the matter of obtaining strain-free windows. The materials tried were: annealed glass, annealed fused quartz, and microscope cover slides. To the present, no material or method of processing has yet been found such that the instrument under consideration cannot detect the presence of extraneous birefringences. To obtain satisfactory windows, large quantities

of these were tested, and the best pairs were selected.

At low concentrations and velocity gradients, the effect of the windows is significantly large when compared to the birefringence of the solutions, which prompted the development of the corrections, formulas (17) and (18), and the refinement of the measurement techniques. The latter were found to be limited by the resolution of the graduate circles and verniers.

To determine the amount of birefringence of the windows and the location of their optic axis, use is made of equations (15). With the Couette cell filled and all windows in place, the position at which the analyzer makes the photoelectric system traverse the null is noted at successive attitudes. The points so obtained describe a sinusoidal curve when plotted versus the attitude of the polarizer. To establish the position of the nodes, i. e., the isoclines of the windows, the analyzer positions  $z_i$  are assumed to be related to a function  $y_i$  of the attitude  $x_i$  :

$$y_i = A + B \sin 2x_i + C \cos 2x_i$$

such that the squared error between the assumed function and the data points is a minimum; that is to say, choosing A, B, and C such that the function

$$\sum_i (y_i - z_i)^2 = F(A, B, C)$$

is a minimum. Differentiating F with respect to A, B, and C, setting the results equal to zero, and solving for A, B, and C, yields the function that best fits the data by the method of least squares. The amount of birefringence and angle of isocline of the windows are then obtained as:

$$\delta_w = (B^2 + C^2)^{\frac{1}{2}}$$

$$\chi_w = \frac{1}{2} \text{arc tan } -\frac{C}{B}$$

In actual practice, the position of the null  $z_1$  is determined at successive intervals of  $10^\circ$ , throughout the  $200^\circ$  that constitute the range of the instrument. The data is then reduced by computer (Burroughs 220) by a fixed program developed for the purpose. For weakly birefringent solutions, particularly at small velocity gradients, the data is gathered by the same method and then corrected for the effect of the windows by means of equations (17) and (18).

It has been found that the measurement of the windows must be made for every experiment, even when a number of runs occur in rapid succession. This is due to the fact that the birefringence of the window changes through time, and that since the windows must be removed at each experiment for cleaning, the positions of their isoclines also change.

In runs where the concentrations and gradients are sufficiently large so that they produce effects much greater than the one of the windows, the simpler and more rapid technique of looking for the null with polarizer and analyzer in quadrature is used.

Since it is not practical to determine the position of the isoclines in the windows at every run, and then establish the quadrature between polarizer and analyzer, setting the polarizer parallel to the axis of the windows so that their effect vanishes, a correction must be made to allow for the small error in quadrature which constitutes the amount of birefringence in the window at the reference location where quadrature is established.

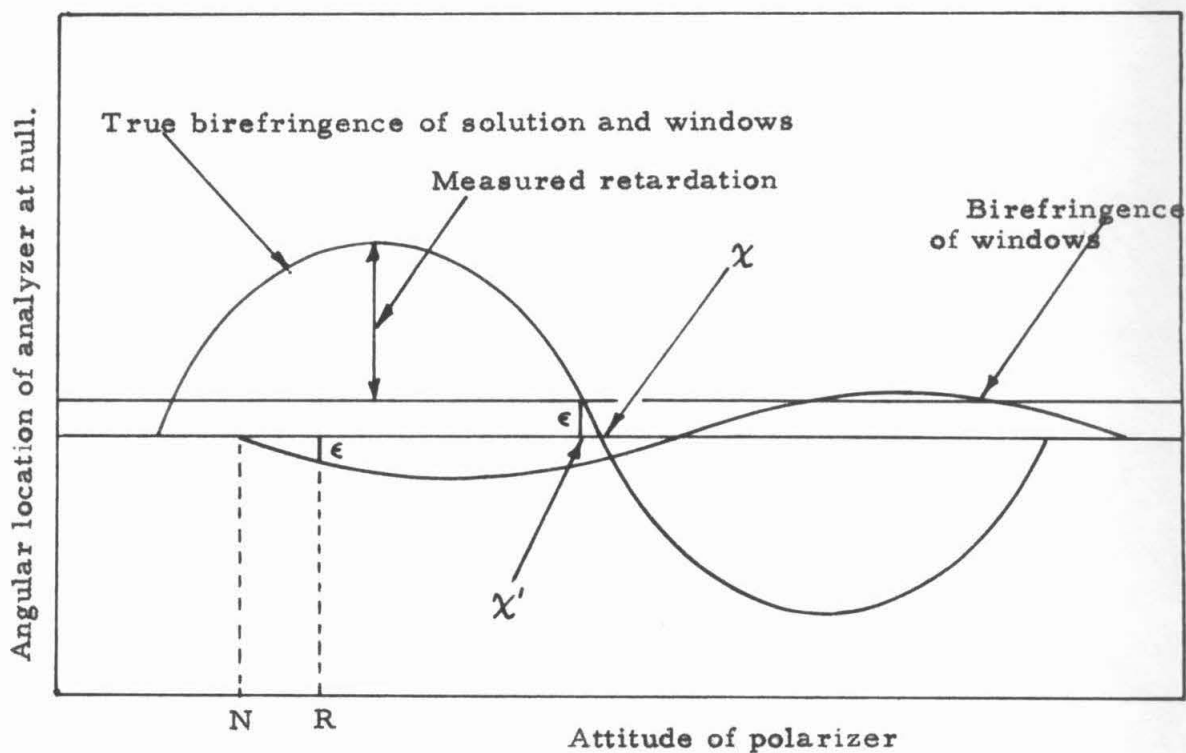


Figure 10. Effect of the error in quadrature  $\epsilon$  on the position of the isocline and the measured amount of retardation.

In this correction, both the birefringences of the combined system of windows plus solution and windows alone are assumed to be represented by sinusoidal functions of the attitude of the polarizer. With reference to Figure 10, the reference attitude  $R$  is chosen so that it is fairly close to the isocline of the window, whose position is not yet available. Setting polarizer and analyzer in quadrature at this position, there will be a small error  $\epsilon$  between the position at which polarizer and analyzer are locked and the true location of quadrature. With reference to Figure 10, when the rotor is set in motion, the solution exhibits its birefringence so that when the null is again sought by rotating the assembly of polarizer and analyzer, this will appear at a location  $\chi'$  where the error due to the window exactly balances the birefringence of the combined system. Once the data for the window is reduced, the error in quadrature becomes available, and the actual position of the isocline of the system is given by the relation:

$$\chi = \chi' - \frac{1}{2} \text{arc sin}(N-R)$$

The amount of SBR must also be corrected for the amount of retardation represented by the error in quadrature between both prisms. Since the error is equivalent to shifting the base line of a sinusoidal curve, the correction is simply additive.

A sample data sheet and the corresponding data reduction and correction are included in the Appendix.

#### IV. EXPERIMENTAL RESULTS

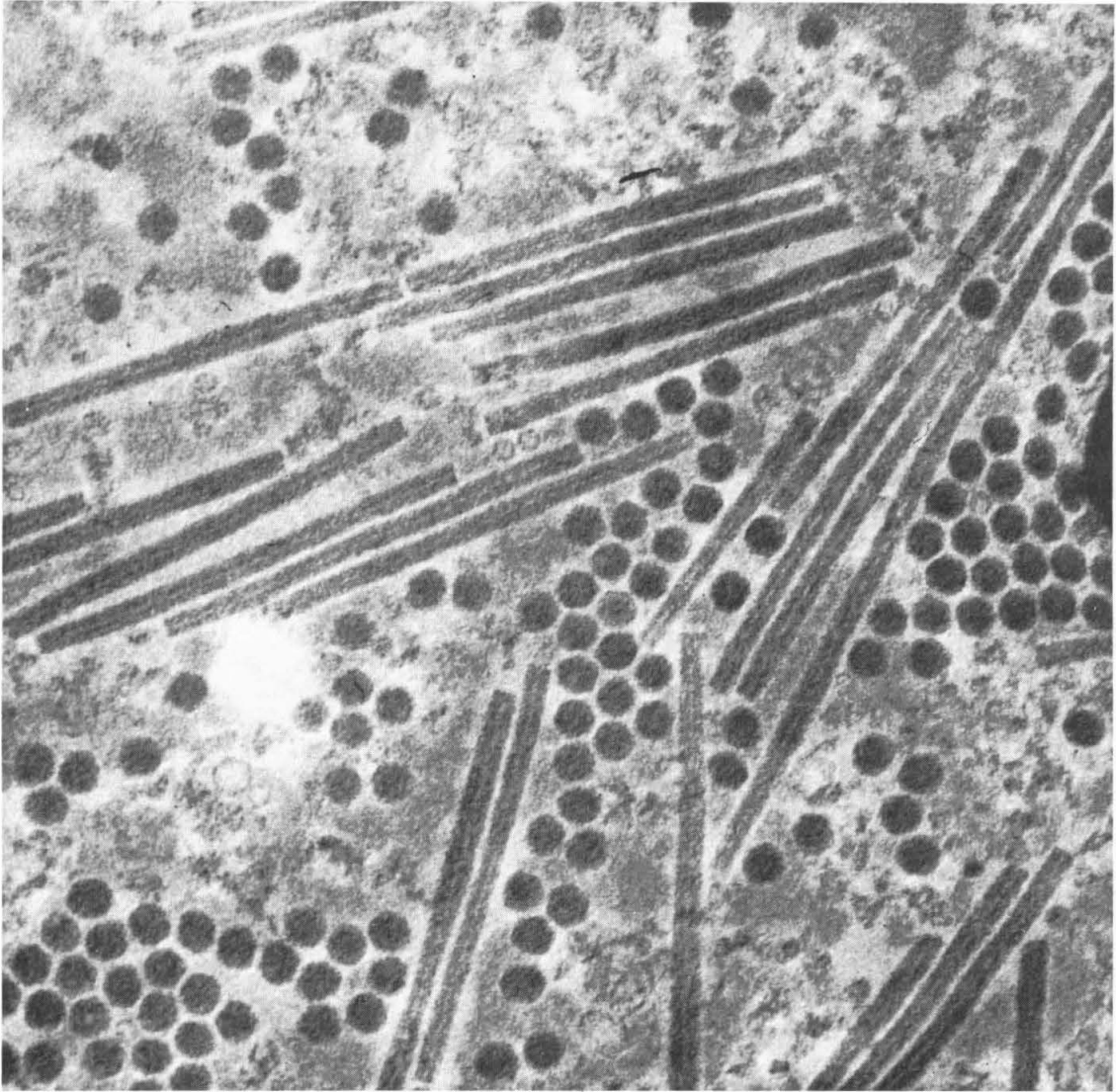
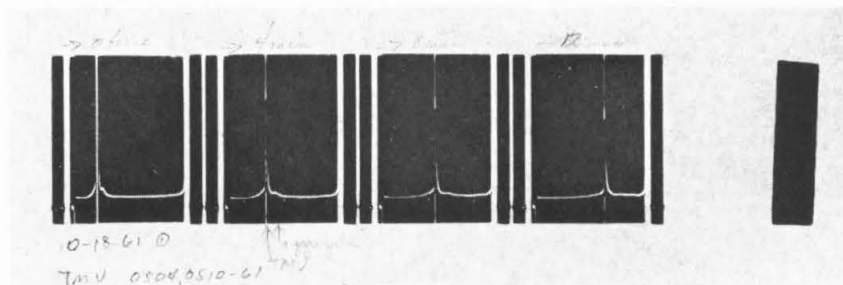
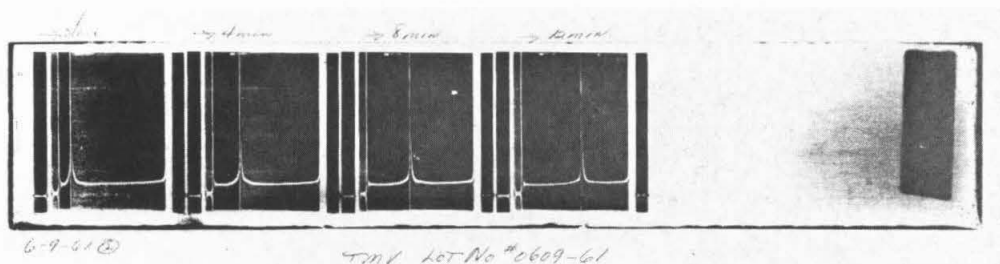


Figure 11. Electron microscope photograph of a mixture of TMV and SBMV. Magnification: 200,000 .



Sample 1. TMV lot 0504, 0510-61 (lot 1), at 0.20 per cent in 0.01 M Versene, pH 7.5, 24,630 RPM, 60° bar. Exposures at speed and at 4 minute intervals thereafter. Some evidence of presence of very small amount of aggregate.



Sample 2. TMV lot 0609-61 (lot 2), at 0.20 per cent in 0.01 M Versene, pH 7.5, 24,630 RMP, 30 mm cell, 60° bar. No evidence of presence of aggregate.

Figure 12. Ultracentrifuge runs on TMV samples.

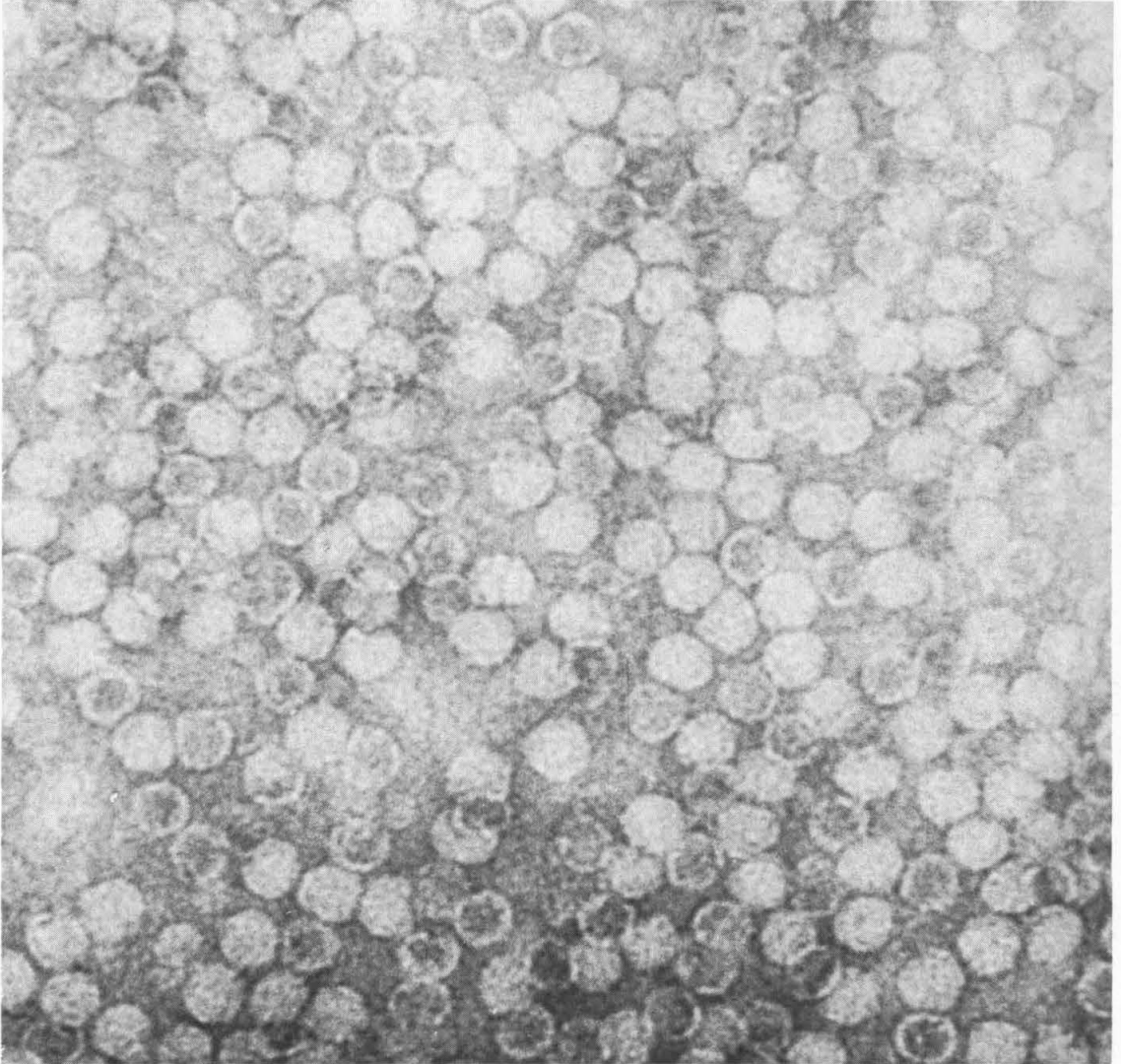


Figure 13. Electron microscope photograph of SBMV. Magnification: 300.000 .

Experimental Results

% TMV by weight	% SBMV by weight	Ratio TMV/SBMV	Retardation per unit velocity gradient Å sec/cm	Viscosity Centipoise
0.375			2.30	1.142
0.275				1.094
0.264			1.61	
0.194			1.16	
0.190				1.066
0.181			1.08	
0.101				1.037
0.096			0.57	
	1.020			1.037
	0.465		none	1.018
	0.244			1.008
	0.121			0.988
0.359	0.123	2.92	2.05	1.142
0.230	0.079	2.91	1.28	1.074
0.101	0.035	2.97	0.58	1.037
0.382	0.382	1.00	2.05	1.133
0.275	0.275	1.00	1.45	1.104
0.333	1.080	0.31	1.85	1.152
0.166	0.540	0.31	0.92	1.070

Note: all experiments were conducted at  $20.00 \pm 0.01$  °C. All solutions in 0.01 M Versene, at pH 7.4 . Viscosity of Versene solution: 0.988 centipoise. All mixtures were made with TMV (lot 2).

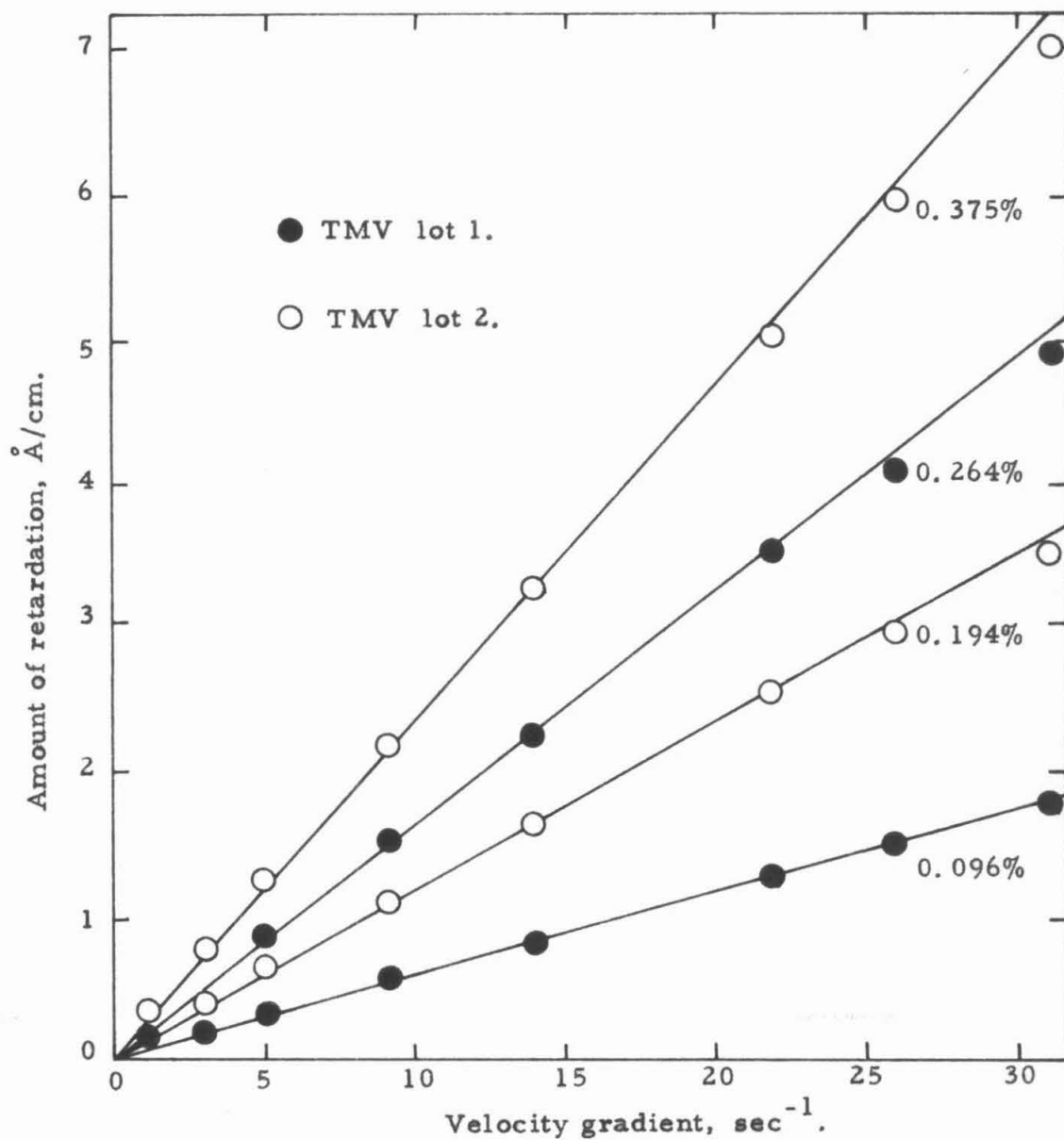


Figure 14. Amount of retardation of solutions of pure tobacco mosaic virus, as a function of velocity gradient, at different concentrations by weight. Concentrations were determined with a Zeiss PMQ II spectrophotometer.

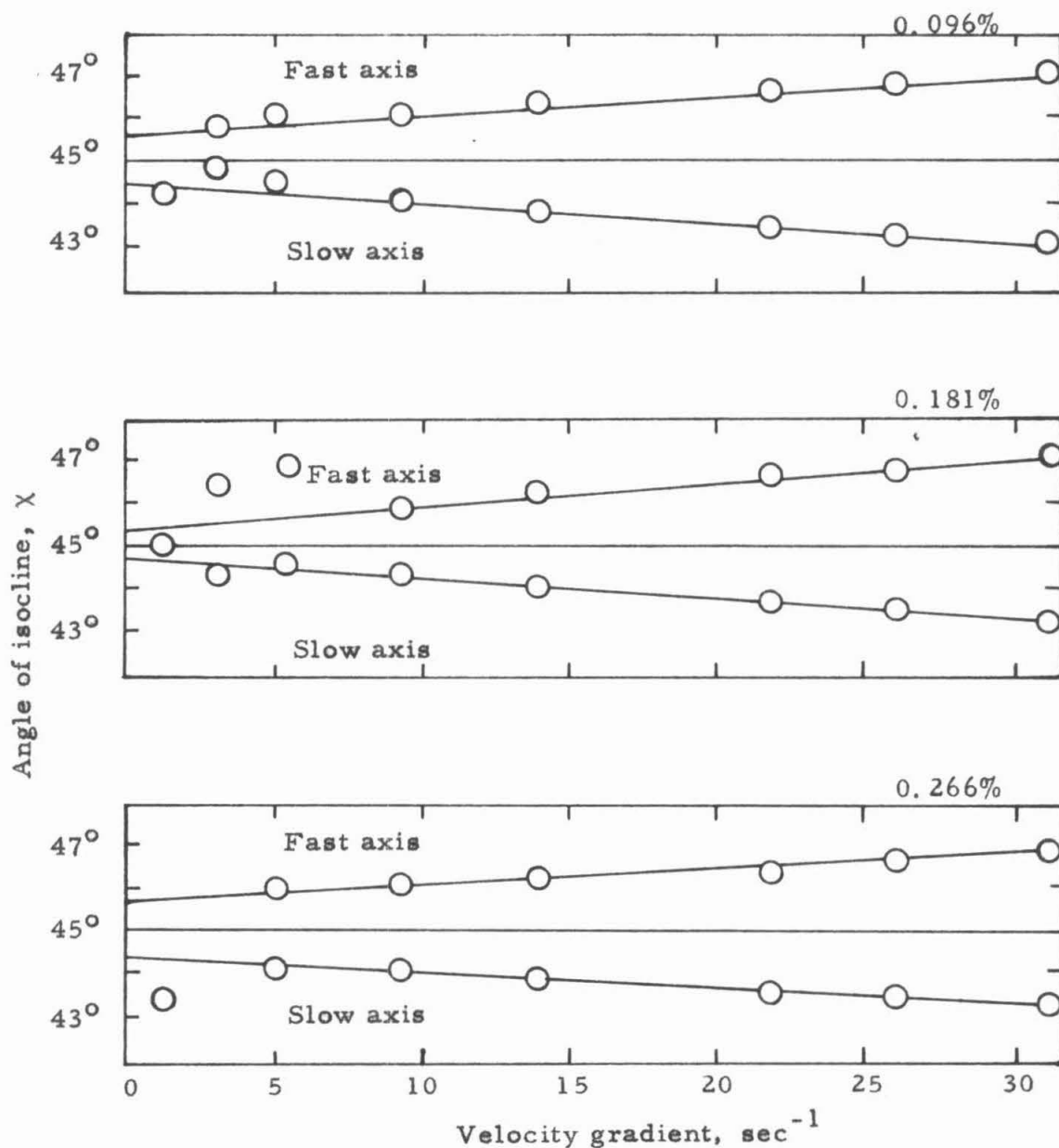


Figure 15. Experimental results. Angle of isocline of solutions of TMV lot 1 as a function of velocity gradient. The stream line is at  $\chi = 0^\circ$ .

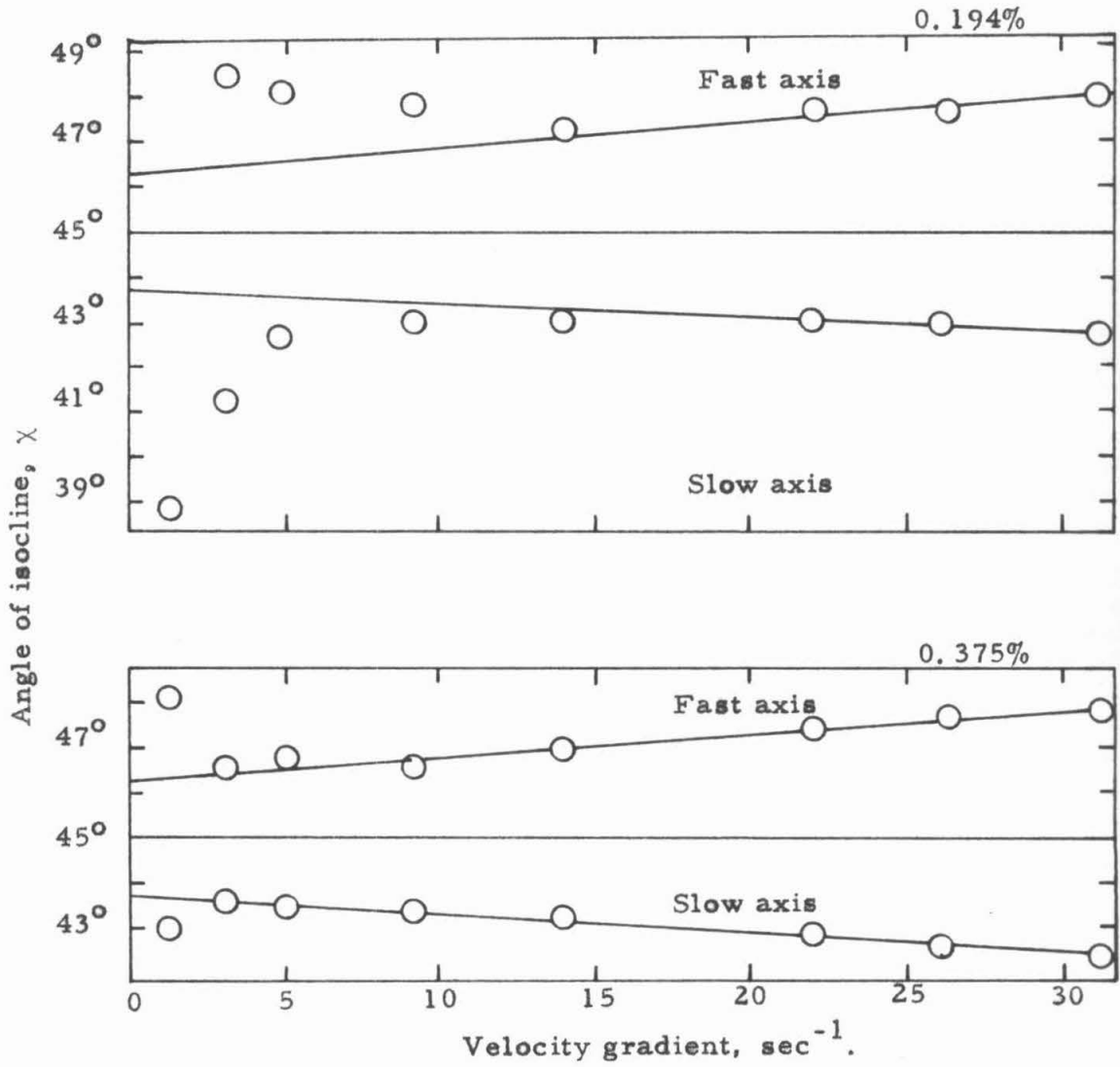


Figure 16. Experimental results. Angle of isocline of solutions of TMV lot 2 as a function of velocity gradient. The stream line is at  $X = 0^\circ$ .

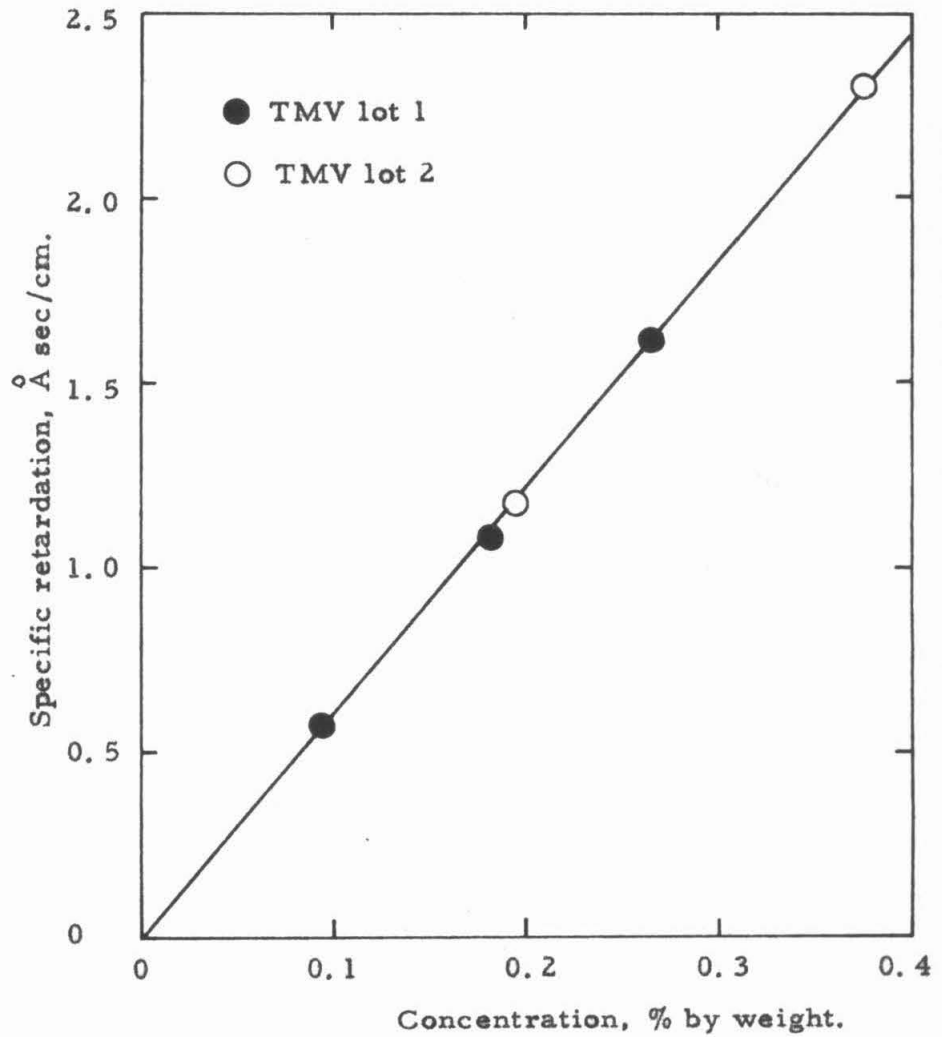


Figure 17. Amount of retardation per unit velocity gradient as a function of concentration of  $TMV_3$  in % by weight, or grams per  $100\text{ cm}^3$ .

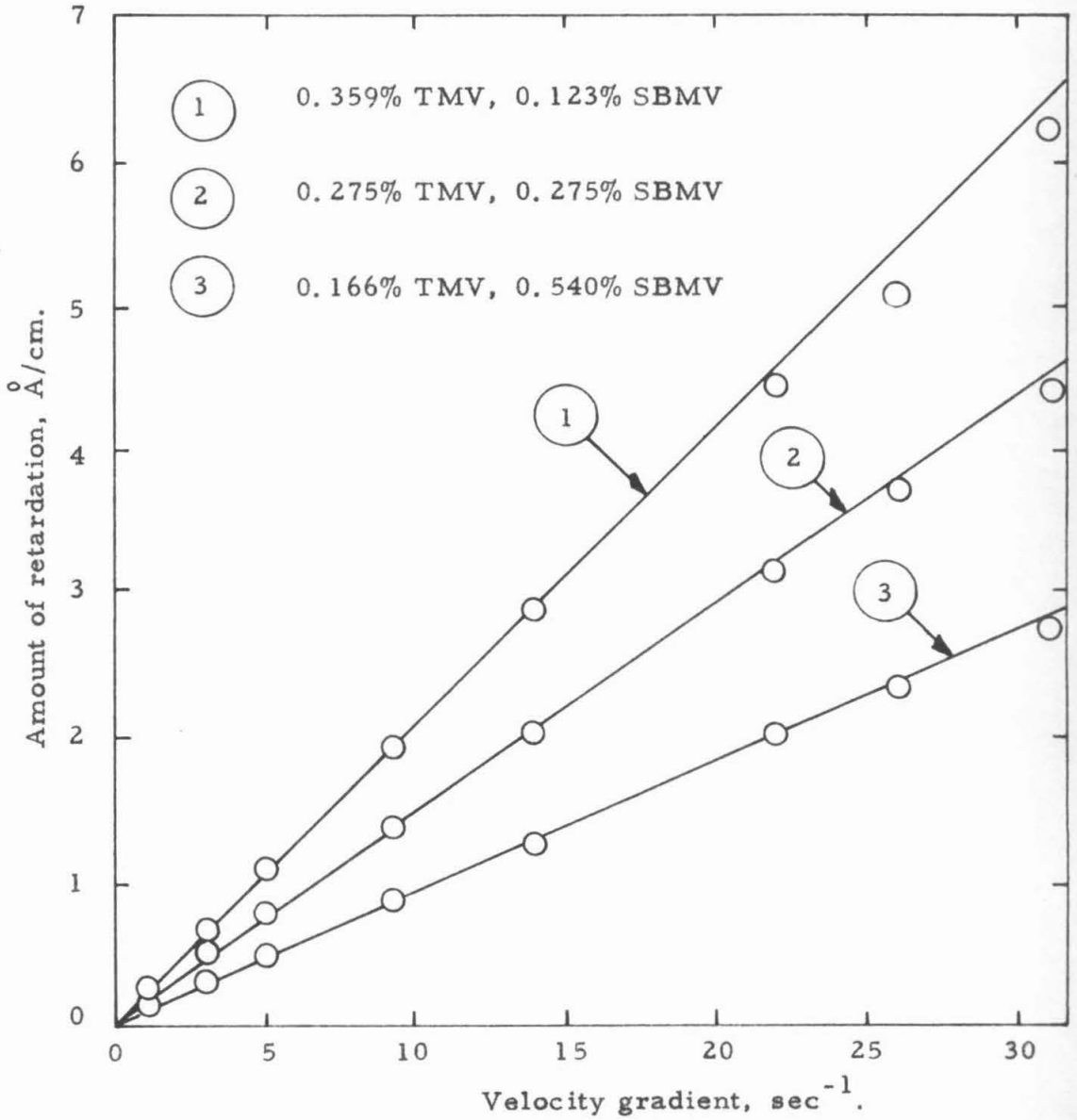


Figure 18. Typical data on the amount of retardation of mixtures of TMV and SBMV as a function of velocity gradient.

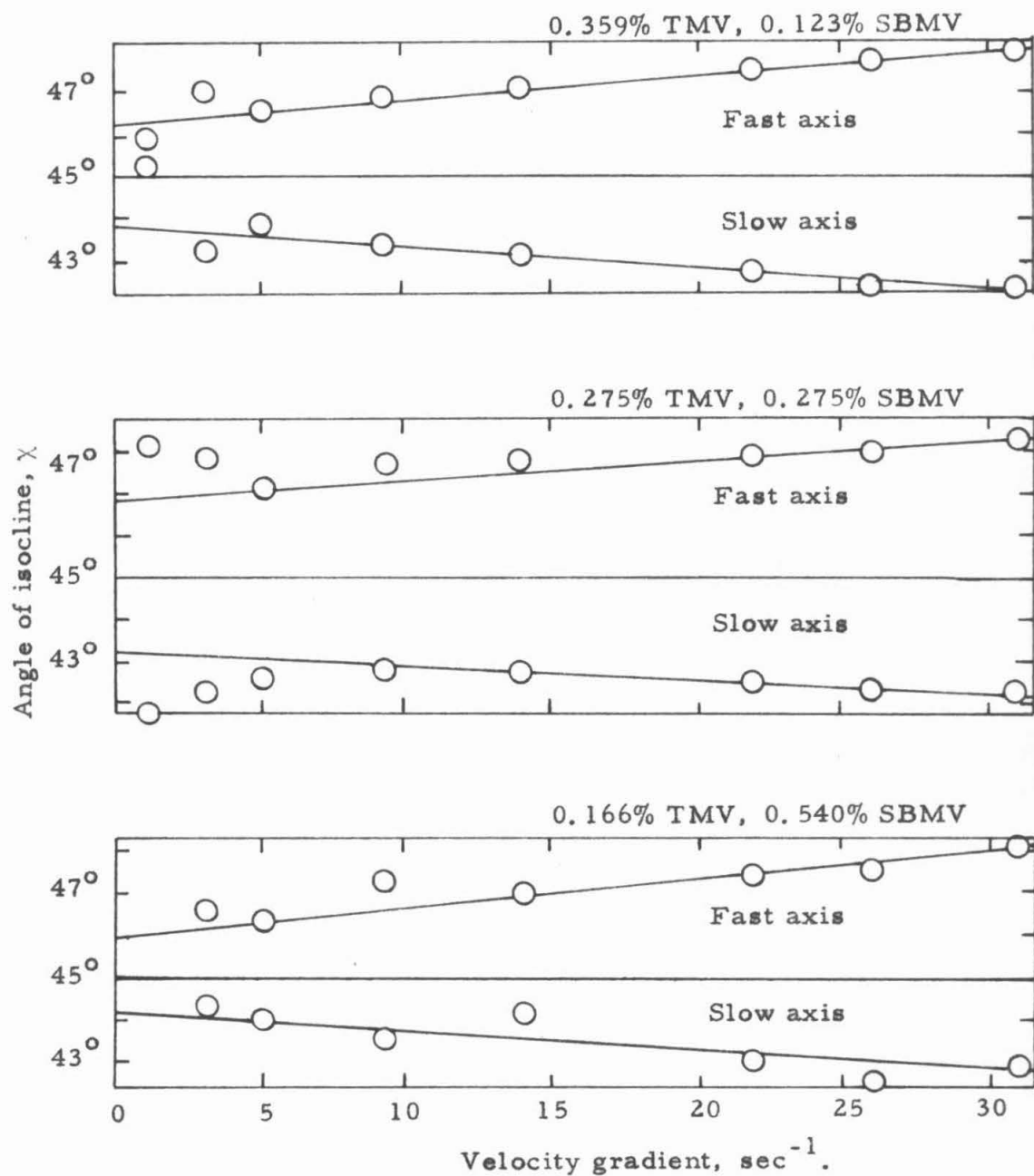


Figure 19. Angles of isocline corresponding to the experiments shown in Figure 18. The stream line as at  $\chi = 0^\circ$ .

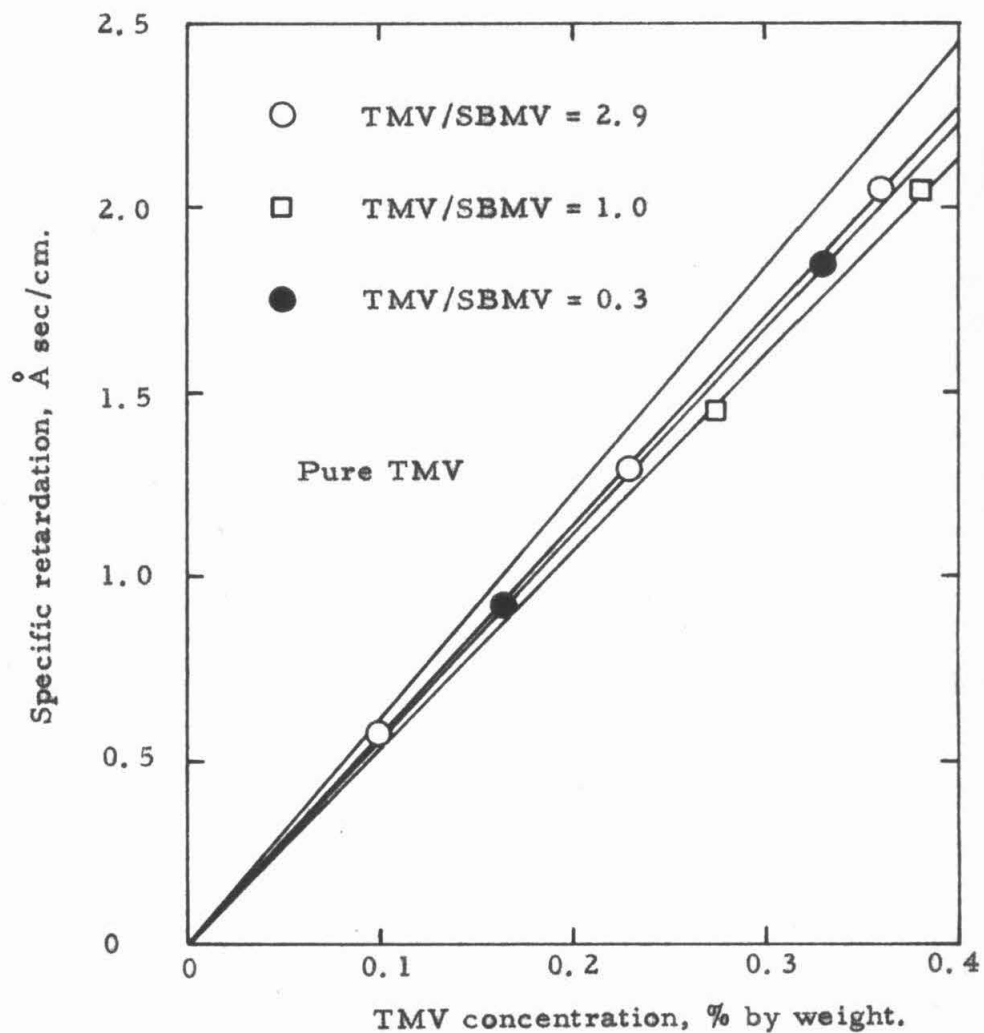


Figure 20. Amount of retardation per unit velocity gradient as a function of concentration of TMV in % by weight, of mixtures of TMV and SBMV. The ratios by weight of TMV to SBMV are indicated. The pure TMV line is obtained from Figure 17.

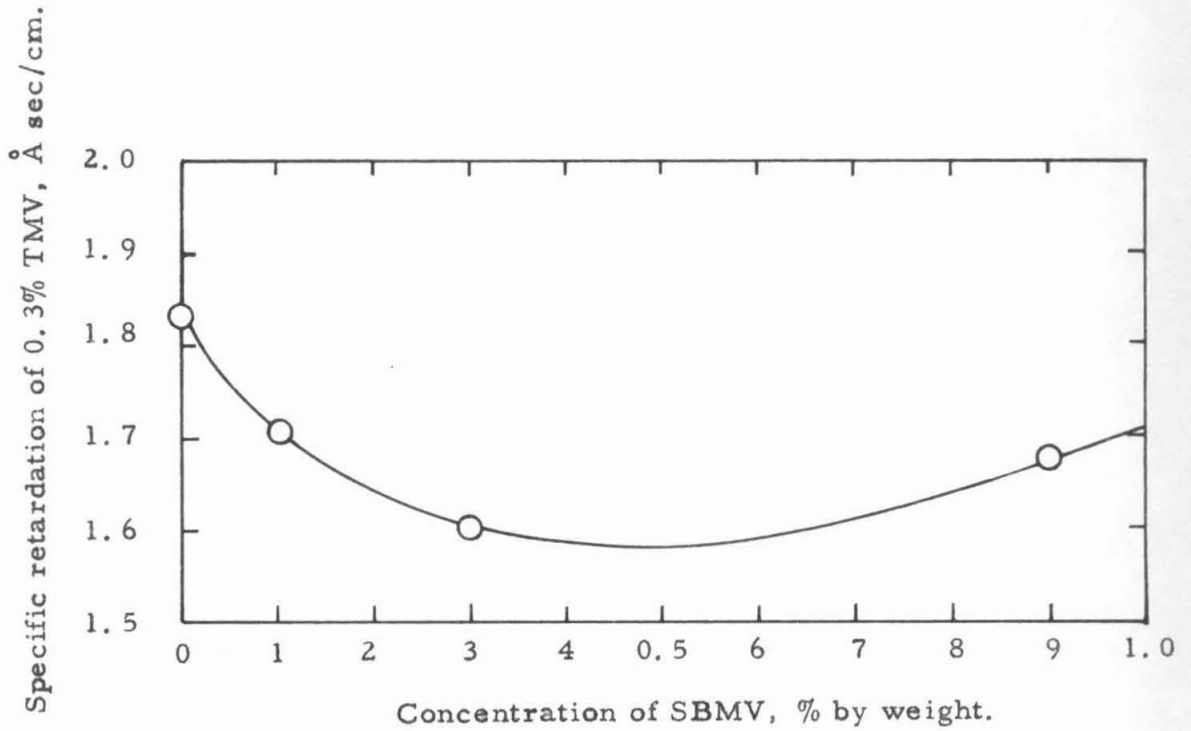


Figure 21. Specific retardation of TMV-SBMV mixtures, at a TMV concentration of 0.3%, as a function of the amount of SBMV in the mixture.

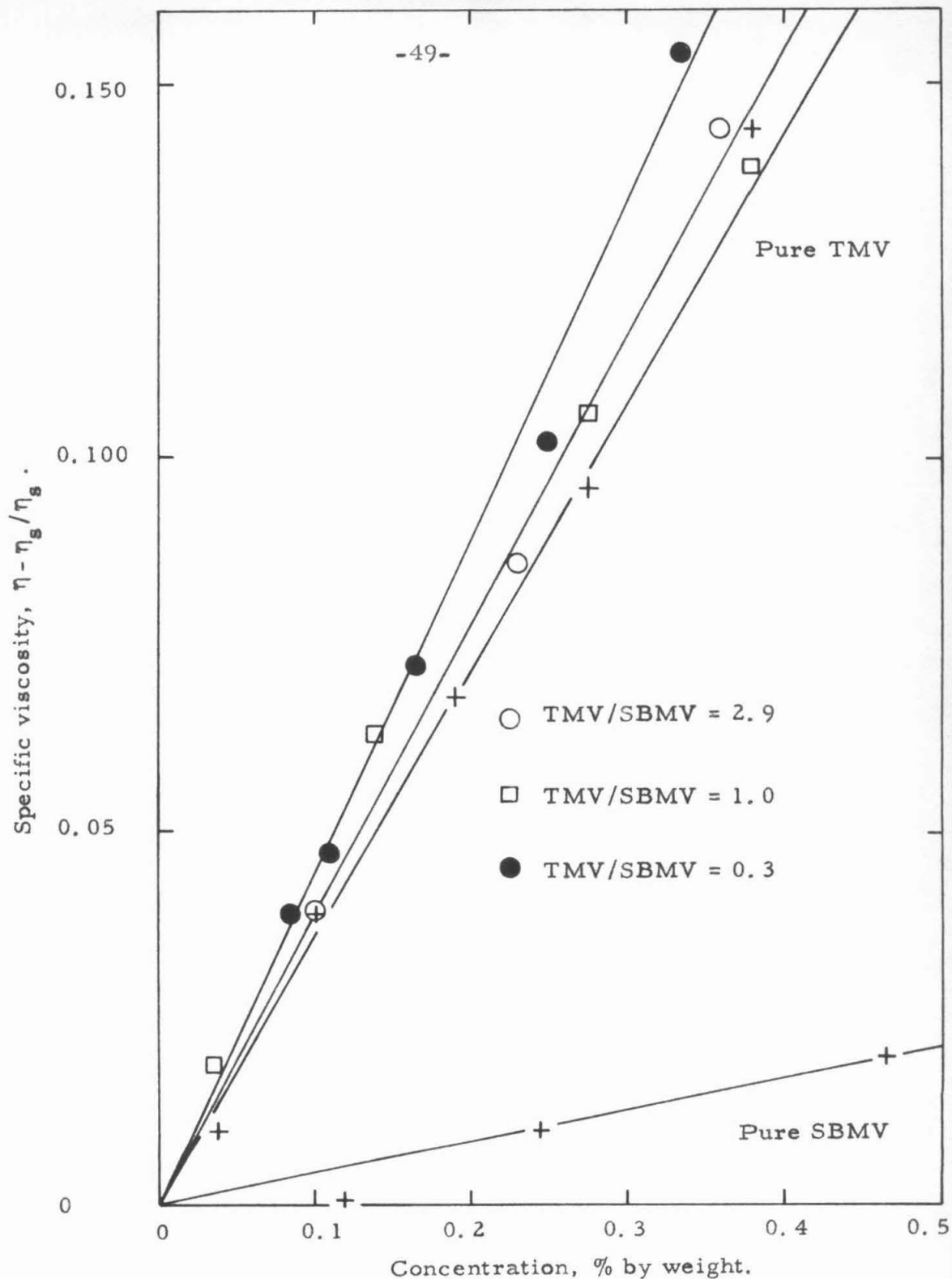


Figure 22. Specific viscosity of TMV, SBMV, and mixtures of TMV and SBMV, as a function of concentration. The viscosity of the solvent (water + versesne)  $\eta_s$  is 0.998 centipoise. The specific viscosity of the mixtures is plotted as a function of the concentration of the TMV.

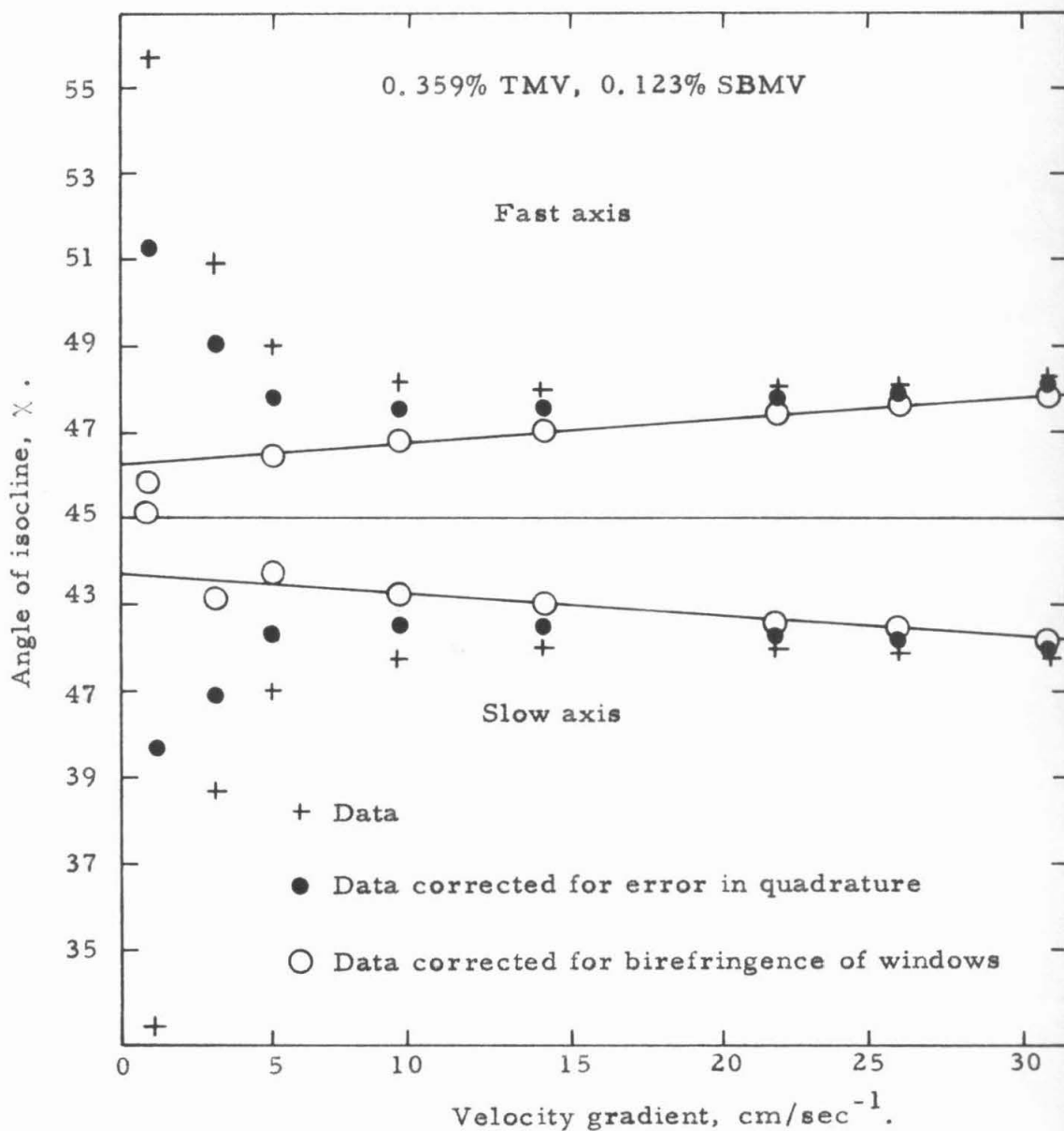


Figure 23. Effect of corrections on the position of the angle of isocline.

## V. DISCUSSION OF EXPERIMENTAL RESULTS AND CONCLUSIONS

Some of the most recent and accurate measurements of the SBR of TMV solutions made by Leray<sup>(9)</sup> indicate that at low shear rates and concentrations, some departures from the results predicted by the Peterlin and Stuart theory appear. Observations show that the angle of isocline, even though it tends towards  $45^{\circ}$  when the velocity gradient approaches zero, does so up to a certain point and then starts leveling off at the lower velocity gradients.

Assuming that the phenomenon is not due to extraneous birefringences, the abnormal behavior of the angle of isocline can be explained by assuming that at the low velocity gradients there exists in the solution a partial structurization of the TMV particles which is broken up at the higher shear rates. This structurization can be produced by weak chemical bonds among the particles, which would tend to form some sort of organization of the material. Evidence of such a phenomenon was found by Hearst and Vinograd<sup>(10)</sup> in experiments made with TMV in the ultracentrifuge, in which the sedimentation behavior was found to be strongly concentration dependent. To explain their results, they tentatively proposed that an alignment is brought about among the macromolecules as a result of chemical interactions among them. In SBR, the result is such that, even though the forces tending to align the particles are small, a number of particles align themselves simultaneously as a unit, the net result being that there is a larger quantity of aligned material, which produces an optical effect equivalent to the one found at the higher shear rates. It must be noted,

though, that if such an effect exists, it must be of such a nature that it does not affect the amount of birefringence, since no evidence of this effect is found in analyzing the data on the amount of birefringence.

To test these ideas, a number of samples of concentrated TMV solutions were obtained from the Department and Laboratories of Nuclear Medicine and Radiation Biology, of the School of Medicine, of the University of California at Los Angeles. These samples were highly monodisperse and very uniform in length, as attested by the ultracentrifuge runs made on them, shown in Figure 12 and the electron microscope photograph shown in Figure 11. These samples were diluted to concentrations ranging from 0.4 per cent to 0.1 per cent by weight, in 0.01 molar Versene at a pH of 7.4. The concentration of each dilution was determined with a Zeiss PMQ II spectrophotometer. A number of determinations of the SBR of these solutions was made at velocity gradients ranging from 0.3 to 31.1  $\text{sec.}^{-1}$ .

The experimental results showed that the amount of SBR of these TMV solutions is linear with velocity gradient, as shown in Figure 14 and as predicted by theory. A small departure from linearity was observed at the higher velocity gradients. These results also confirm that the amount of specific SBR, defined as the amount of retardation per unit velocity gradient, is linear with respect to concentration, as shown in Figure 17.

Concerning the angle of isocline, no satisfactory proof was obtained to substantiate the claim that a departure from the Peterlin and Stuart theory exists at low velocity gradients. It was indeed observed that a departure exists if the data is plotted directly, as shown in Fig-

ure 23 where a representative case is shown, but this departure disappears when the corrections for the error in quadrature and the birefringence of the window are applied.

The position of the streamline with respect to which the  $45^\circ$  location is established was always determined by averaging the position of the isoclines of the fast axis of the solution in the clockwise direction of rotation, and the slow axis in the counterclockwise direction of rotation. This method yields the position of the streamline to a degree of accuracy comparable to the one of the determination of the isocline, which is estimated to be of the order of  $\pm 0.10^\circ$  at the lower velocity gradients. It has always been observed that in linearly extrapolating the isocline to zero shear, the value for zero shear always falls short of the  $45^\circ$  value predicted by the theory, the discrepancy being most severe in those cases where the isocline departs more radically from the predicted monotonic approach to the  $45^\circ$  value. This behavior is considered to be due to effects of extraneous birefringences not accounted for in the simplifications made to arrive at a directly applicable correction.

In view of these results, it is apparent that further refinements of the measuring techniques will be possible if a method is found for eliminating the extraneous birefringences of the windows. Due to this, consideration is being given to an apparatus to be built in which the liquid samples are contained in place by the surfaces of the optical elements such as the polarizer and the quarter-wave plate, in order to eliminate as many sources of stray birefringence as possible.

Taking into account the difficulties introduced by extraneous birefringences, the data of the SBR of the TMV solutions was found to

permit determinations of the angle of isocline accurate to one degree for a retardation per unit length of  $1 \times 10^{-9}$ . As a comparison, a typical instrument for SBR studies, such as the one built by the Rao Instrument Company, yields accuracies of the order of one degree per  $7.5 \times 10^{-8}$  relative retardation as described by Edsall, Rich, and Goldstein<sup>(11)</sup>, and the same Rao instrument modified for photoelectric observation by Zimm<sup>(12)</sup> only increases the accuracy to one degree per  $7 \times 10^{-9}$  relative retardation.

In view of the above results, it was decided to apply the information obtained on the SBR of TMV, and the measuring technique developed, to the question whether for dilute solutions for which existing theories are supposed to be valid, there are significant hydrodynamic interactions among particles which might explain the discrepancies observed between different methods for characterizing macromolecules, such as viscometry, SBR, sedimentation, and transient Kerr effect.

That hydrodynamic interactions might contribute significantly to the macroscopic characteristics of dilute solutions of submicroscopic particles was proposed by Collins and Wayland<sup>(13)</sup> to explain the viscosity behavior of mixtures of TMV and polystyrene latex spheres, (PSL), as a function of the concentration of both particles. In the first phase of the experimental program of which this study is a part, they found that the specific viscosity of mixtures of TMV and PSL was higher than that predicted by the simple addition of the specific viscosities of the components by a term proportional to the product of the concentrations of the two particles. In explaining this result, they proposed that the presence of the spheres interferes with the tendency

of the rods to assume an orderly rotational motion in shear flow which leads to an increase in viscosity.

If the orderly rotational motion of the rod-like particles is tampered with by a random hydrodynamic interaction, such as the one that would be produced by the presence of spheres, a decrease of the SBR of the mixture with respect to the SBR of pure TMV solutions at the same concentration should be observed, since no direct contribution to the SBR of the mixture can be expected from the spherical particles, which show no optical asymmetry regardless of orientation in shear flow.

To see what information could be obtained from mixtures of TMV and spherical particles, it was decided to use a spherical virus compatible with TMV, since the PSL had proven to have a surface chemistry that had produced considerable difficulties in previous experiments, and furthermore was so large that it would have scattered too much light for good optical experiments. The choice fell upon southern bean mosaic virus (SBMV), which is a spherical virus of  $2.52 \times 10^{-6}$  cm diameter.

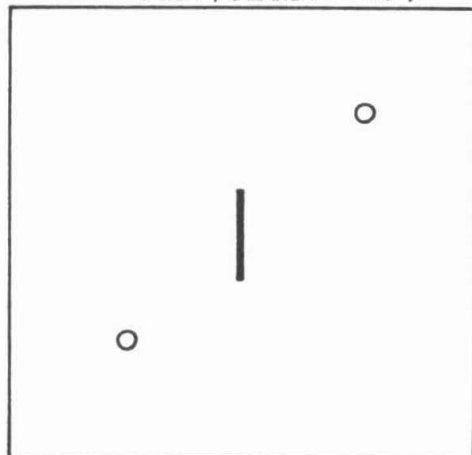
A program was started in the laboratory to secure this virus by planting a number of southern bean plants and infecting their leaves with an available sample of the virus. After an appropriate time, the leaves were collected and the virus extracted according to the technique described by Konrad<sup>(14)</sup>. Electron microscope photographs of the obtained virus show that it is quite pure, as can be seen in Figure 13. The presence of some particles that have a dark center is attributed to an artifact of the electron microscope.

The two viruses were mixed in such proportions as to obtain three main sets of solutions where the proportion by weight of TMV to SBMV was respectively 3:1 , 1:1 , and 1:3 , at a nominal TMV concentration of 0.3 per cent by weight. Experiments were made at the original concentrations and at dilutions of the original mixtures.

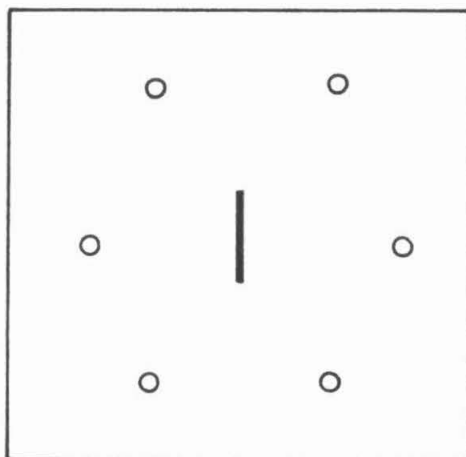
To interpret the information obtained from these experiments, attention must first be given to the theoretical results given by equation (A60), which predicts that the amount of retardation is a linear function of the viscosity felt by the particle. This viscosity, according to the best present theories, seems to lie somewhere between the viscosity of the matrix fluid and that of the solution. That the amount of SBR is a linear function of the viscosity was checked experimentally by Sutera (loc. cit. ), who purposely altered the viscosity of the solvent by using an 85 per cent glycerine solution for the matrix fluid, which, at 20°C, is approximately 100 times as viscous as water. He observed a ten-fold increase in the amount of SBR for equivalent concentrations and velocity gradients. That the observed increase is not of the same order of magnitude of the increase in viscosity is explained by the fact that the amount of SBR also depends on the difference in index of refraction between the particle and the matrix fluid. The lesser the difference the less marked the effect, as in this case, where the index of refraction of the mixture of glycerine and water is considerably higher than the one of water, which results in a smaller difference with the index of refraction of the particle, and thus a smaller effect.

It should further be noted that the addition of a small number of rigid spheres to a Newtonian fluid increases the relative viscosity of

TMV/SBMV = 2.9



TMV/SBMV = 1.0



TMV/SBMV = 0.3

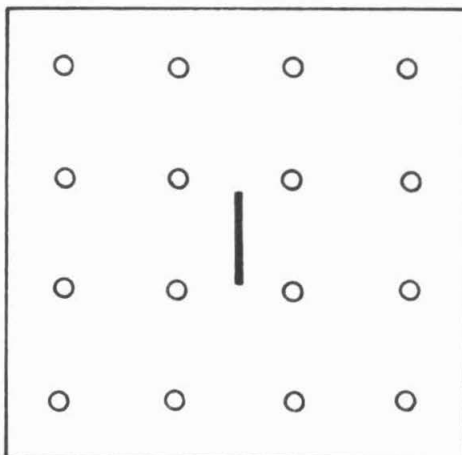


Figure 24. Scale diagram of the relative proportions and sizes between particles in the mixtures of TMV and SBMV used, for a constant TMV concentration of 0.3% by weight.

the mixture in a manner proportional to the volume fraction occupied by the spheres, as predicted by Einstein<sup>(15)</sup> in a linear theory where second order effects are neglected. This consideration strongly suggests that if no other mechanisms are present, the SBR of mixtures of rods and spheres would be greater the larger the concentration of spheres - for equal concentrations of rods - because of the increased viscosity of the suspending matrix fluid. As shown in Figures 20 and 21, the experimental evidence shows that the opposite effect takes place.

To analyze the result obtained, attention must be given to the relative sizes and quantities of particles present. The most recent studies on TMV made by Boedtker and Simmons<sup>(16)</sup> indicate that its molecular weight is  $39.0 \times 10^6$  and that its dimensions are  $3.00 \times 10^{-5}$  cm length by  $1.80 \times 10^{-6}$  cm diameter. Thus, at a concentration of 0.3 per cent by weight, and at room temperature, there will be approximately  $4.63 \times 10^{13}$  particles per  $\text{cm}^3$ .

The molecular weight of SBMV is  $6.63 \times 10^6$ , according to Miller and Price<sup>(17)</sup>. Therefore, in a 3:1 mixture of TMV and SBMV, when the concentration of TMV is 0.3 per cent by weight, there are approximately  $8.98 \times 10^{13}$  particles per  $\text{cm}^3$ , or twice as many particles of SBMV as of TMV.

Referring to Figure 24, where relative sizes and proportions of these particles are shown to scale for the three ratios used, it is proposed that at the 3:1 ratio of TMV to SBMV the TMV particle essentially ignores the effect of the addition of spheres to the bulk viscosity of the matrix fluid and moves according to hydrodynamic forces governed by the viscosity of the pure solvent in its immediate surroundings.

The decrease in SBR is then due to the random interaction between the hydrodynamic fields surrounding both species of particles. Since the translational movement of the SBMV can be considered to be completely random, the interaction appears as a tendency towards disturbing the orderly rotation of the rods, and thus as a decrease in SBR. This effect seems to be linear with concentration when the relative proportions of the particles are maintained. This interpretation of the results corroborates qualitatively the findings of Collins and Wayland (loc. cit.).

To further test these conclusions, the experiments with the 1:1 and the 1:3 ratios by weight were carried out. For the 1:1 mixture it was found that the SBR decreased further, while for the 3:1 ratio the trend reversed itself. This last result is particularly significant, since at this proportion of the mixture there are approximately 16 SBMV particles per particle of TMV, and very likely the TMV particle can no longer ignore the increase in bulk viscosity of the matrix fluid produced by the presence of the spheres. These results are shown in Figure 21 where the specific SBR is plotted as a function of the concentration of SBMV for a constant TMV concentration of 0.3 per cent by weight.

Since these results depend somewhat on the nature of the viscosity of these mixtures, their viscosities were measured at the laboratory of Professor E. W. Merrill at the Department of Chemical Engineering of the Massachusetts Institute of Technology, where an instrument has been developed and built that is able to measure the viscosity of small samples of the order of  $2 \text{ cm}^3$  at the velocity gradients characteristic of these experiments, i. e., from 0.3 to  $30.0 \text{ sec.}^{-1}$ .

The results obtained from these measurements are shown in

Figure 22. It can be seen that within the accuracy of the technique, no anomalies appear in the viscosity of either the pure TMV and SBMV or the mixtures of both, which seems to have a viscosity roughly equal to the sum of both viscosities.

The above interpretation of the results is qualitative and presents some difficulties. It can be argued that since the hydrodynamic effect of the SBMV is random, the net effect that it would have on the orderly rotation of the TMV would average out to zero. To see whether this is the case, it should be pointed out that simultaneous interactions that cancel each other are a very unlikely event in the present system. Secondly, for the net effect of the interaction of the spheres to cancel out, the number of particles that are knocked out of the orderly rotation should be exactly balanced by an equal number of particles which, being in a random state of motion due to the Brownian motion of the surrounding fluid, are knocked precisely into orderly rotation. Qualitatively, it appears that all random interactions with oriented particles are unfavorable events, and that only a small number of random interactions with randomly oriented particles are favorable events; as a whole, the unfavorable disorienting effect is predominant.

A second consideration is thermodynamic in nature. If the net effect of the presence of the SBMV is to increase the randomness of the rotational motion of the rods, the average rotational kinetic energy of these would have to increase at the expense of the kinetic energy of the spheres. This is equivalent to saying that the net effect is to "heat" the TMV particle while "cooling" the SBMV particle, which is in contradiction to the Second Law of Thermodynamics. In analyzing this

concept, it must first be pointed out that such an argument applies thermodynamic laws to single particles of a system constituted by a very large number of interacting particles. If thermodynamic considerations are applied to the analysis of the results, it is the total entropy of the system that should be considered. Considering the entropy of the pure TMV solution to be a measure of the order in the system, it is found that the addition of the spheres increases the disorder of the system, and the system passes from a state of comparatively low entropy, in which a significant number of particles have ordered rotational motion, to a state of higher entropy where a lesser number of particles possess this order. Since this is the direction in which natural phenomena occur, it should be concluded that the system passes from a low probability state to a higher probability one, and thus no violation of the Second Law occurs.

In trying to reconcile the apparent increase in the temperature of the TMV particle at the expense of the energy of the spherical particle with the above consideration, the complete system must be analyzed. First it must be noted that the total kinetic energy of the rod need not change because of the random interaction, but as an alternative, a redistribution within its various degrees of freedom could take place. It must also be considered that a certain amount of mechanical energy is expended in keeping the rods aligned. If the spheres act as obstacles to this alignment, the mechanical energy expended will appear directly as thermal energy, which would be another source for the energy that the TMV rod has to acquire if its average rotational kinetic energy must increase. In a sense, it would seem that the oriented

TMV particle is in a "colder" state which is brought to temperature through the action of the spheres.

An altogether different mechanism could also account for the observed results. If it is accepted that there is a certain amount of structurization in the pure TMV solution, it is possible that the Brownian motion of the spheres will break it up. Without going into the question of what would be the optical properties of the structurized material, it is clear that the larger the aggregation, the heavier the unit that moves as a whole, and thus the less the effect of the Brownian motion of the surrounding fluid. This results in greater ease of alignment. If a structurization exists, it should also be broken up at the higher velocity gradients and a departure from linearity of the amount of SBR should be observed. This is indeed the case, as can be seen in Figure 14; however, the same effect is observed in the solutions of mixtures of TMV and SBMV, and thus the argument does not seem to be conclusive.

In concluding, it should be remarked that both viscosity and SBR experiments indicate that the explanation of the effects can be found by considering the hydrodynamic interactions between the particles. On the other hand, ultracentrifuge studies on these systems put in evidence anomalies that could be due to structurization. It is most likely that both phenomena are present, together with other effects, such as electrostatic forces between the particles, which are not put in evidence by these experiments. In view of this, it is very likely that additional information could be obtained from studies such as the transient Kerr effect and the combination of SBR and the Kerr effect.

APPENDIX A

Theoretical Derivation of the SBR of a Solution  
of Long Slender Rods

APPENDIX A

THEORETICAL DERIVATION OF THE SBR OF A SOLUTION  
OF LONG SLENDER RODS

A. 1 Motion of a Particle According to Hydrodynamic Theory.

The theoretical description of the hydrodynamic behavior of small particles was derived by Jeffrey<sup>(18)</sup> for the general case of an ellipsoid, and solved in detail for a linear velocity gradient flow configuration.

In applying the Navier-Stokes' equation to the motion of small particles with small velocities, attention must first be given to the relative size of the particles. Accordingly, the minimum dimension of the particle must be sufficiently larger than the one of the molecules of the fluid in which it is immersed, so that the fluid can be treated as a continuum hydrodynamic medium.

To simplify the equations and boundary conditions, velocities are assumed to be small, so that inertia terms can be neglected, and concentrations are assumed to be small, so that the disturbances in the flow field due to the presence of a particle do not extend to neighboring particles. The particles are also assumed not to have any tendency towards aggregation, i. e., it is assumed that no forces act among them.

The motion of the fluid is assumed to be steady and varying in a scale that is large compared with the dimensions of the particles. Under this condition, a particle immersed in this flow field will assume the velocity of translation of the fluid that it displaces, and its linear motion will be uniform.

Expressing the undisturbed velocity of the fluid in the region surrounding a particle in terms of a Maclaurin's series expanded about the origin of coordinates, each velocity component  $u_i$  is given by the following expression:

$$u_i = u_{i0} + \sum_j \frac{\partial u_i}{\partial x_j} x_j + \sum_j \frac{\partial^2 u_i}{\partial x_i \partial x_j} x_i x_j + \dots$$

Since the particle is assumed to be small compared with the scale of variation of the motion in the fluid, the second and higher degree terms are assumed negligible in the vicinity of the particle. The undisturbed motion of the fluid is then given by the following system of equations:

$$u_i = u_{i0} + \sum_j \frac{\partial u_i}{\partial x_j} x_j \quad (i = 1, 2, 3 ; j = 1, 2, 3) .$$

By the following algebraic manipulation:

$$u_i = u_{i0} + \frac{1}{2} \sum_j \left( \frac{\partial u_i}{\partial x_j} + \frac{\partial u_j}{\partial x_i} \right) x_j + \frac{1}{2} \sum_j \left( \frac{\partial u_i}{\partial x_j} - \frac{\partial u_j}{\partial x_i} \right) x_j ,$$

the strain and rotation components of this motion are identified. Since the scale of the phenomenon is small, all differential coefficients are assumed constant and abbreviated as

$$e_{ij} = \frac{1}{2} \left( \frac{\partial u_i}{\partial x_j} + \frac{\partial u_j}{\partial x_i} \right) = \text{shear strain} = e_{ji}$$

$$r_{ij} = \frac{1}{2} \left( \frac{\partial u_i}{\partial x_j} - \frac{\partial u_j}{\partial x_i} \right) = \text{rotation} = -r_{ji}$$

and the motion of the fluid is given by

$$U_i = u_{i0} + \sum_j e_{ij} x_j + \sum_j r_{ij} x_j$$

or

$$\underline{u} = \underline{U} - \underline{u}_0 = [e_{ij} + r_{ij}] \underline{x} = [A] \underline{x} \quad (A1)$$

where

$$e_{ij} + r_{ij} = a_{ij} .$$

Let  $x'_1, x'_2, x'_3$  be a system of cartesian coordinates fixed to the axis  $a_1, a_2, a_3$  of a particle and moving with it. The surface of the particle (assumed to be an ellipsoid) will be described by:

$$F(x'_1, x'_2, x'_3) = \frac{x'^2_1}{a_1^2} + \frac{x'^2_2}{a_2^2} + \frac{x'^2_3}{a_3^2} - 1 = 0 . \quad (A2)$$

The axes  $x'_1, x'_2, x'_3$  rotate with speeds  $\omega'_1, \omega'_2, \omega'_3$  with respect to the  $x_1, x_2, x_3$  system of coordinates fixed in direction in the fluid but moving with it. The equations of motion in the rotating system are then of the form

$$\mu \nabla^2 u'_i - \frac{\partial p}{\partial x'_i} = \rho \left( \frac{\partial u'_i}{\partial t} - \omega'_k u'_j + \omega'_j u'_k \right) \quad (A3)$$

where  $\mu, \rho,$  and  $p$  are respectively the viscosity, density, and mean pressure in the fluid. The spins  $\omega'_i$  are the components of the vorticity in the fluid, produced by the motion of the fluid which causes the particles to rotate. They are of the form

$$\omega'_i = \left( \frac{\partial u'_k}{\partial x'_j} - \frac{\partial u'_j}{\partial x'_k} \right) ;$$

therefore, the products  $(\omega'_j u'_k)$  are of the order of the squares of the velocities, and are again neglected. After this simplification, the equations of motion reduce to:

$$\mu \nabla^2 u_i' = \frac{\partial p}{\partial x_i'} \quad \text{and} \quad \sum_i \frac{\partial u_i'}{\partial x_i'} = 0. \quad (\text{A4})$$

A solution of this system of equations must now be found such that it agrees with equation (A1) at a large distance from the origin, and that reduces to

$$u_i' = w_j' x_k' - w_k' x_j' \quad (\text{A5})$$

on the surface of the ellipsoid.

Since the boundary conditions are specified on the surface of the ellipsoid, the solution for the potential will be sought in an ellipsoidal system of coordinates. Following Bateman<sup>(19)</sup>, a system of coordinates related to the equation

$$\sum_s^3 \frac{x_s^2}{(a_s^2 + \tau)} = 1$$

is used, where the  $x_s$ 's are rectangular cartesian coordinates;  $\tau$  is a variable parameter; and  $(a_s^2 + \tau)$  are the squares of the semi-axes of a general ellipsoid.

In order to solve Laplace's equation, the following function is constructed:

$$F(\tau) = 1 - \sum_s^3 \frac{x_s^2}{a_s^2 + \tau} = \frac{P(\tau)}{Q(\tau)} \quad (\text{A6})$$

where

$$P(\tau) = \prod_i^3 (\tau - \xi_i)$$

$$Q(\tau) = \prod_i^3 (\tau + a_i^2)$$

and where the  $\xi_i$ 's are the roots of equation (A6) and constitute the elliptical coordinates. Noting that

$$x_s^2 = - \frac{P(-a_s^2)}{\frac{\partial}{\partial \tau} Q(-a_s^2)} \quad (A7)$$

the element of length given by

$$ds^2 = \sum_s^3 dx_s^2$$

can be found as a function of the  $\xi$ 's by using equation (A7). This yields:

$$ds^2 = \frac{1}{4} \sum_s^3 \frac{P(-a_s^2)}{\frac{\partial}{\partial \tau} Q(-a_s^2)} \left[ \sum_p^3 \frac{d\xi_p}{\xi_p + a_s^2} \right]^2 \quad (A8)$$

The cross product terms of the form  $(d\xi_p d\xi_q)$  vanish, and equation (A8) reduces to

$$ds^2 = \frac{1}{4} \sum_p^3 \frac{\frac{\partial P}{\partial \tau}(\xi_p)}{Q(\xi_p)} d\xi_p^2$$

from which it follows that the metric coefficients are:

$$h_p = \left[ \frac{\frac{\partial P}{\partial \tau}(\xi_p)}{Q(\xi_p)} \right]^{\frac{1}{2}}$$

In the  $\xi_p$  system of coordinates, Laplace's equation can now be written as:

$$\nabla^2 \Omega = 4 \sum_p^3 \frac{Q^{\frac{1}{2}}(\xi_p)}{P(\xi_p)} \frac{\partial}{\partial \xi_p} \left[ Q^{\frac{1}{2}}(\xi_p) \frac{\partial \Omega}{\partial \xi_p} \right] \quad (A9)$$

which has a solution for

$$Q^{\frac{1}{2}}(\xi_p) \frac{\partial \Omega}{\partial \xi_p} = \text{constant}$$

and a general solution of the form:

$$\Omega = -C \int_{\xi_p}^{\infty} \frac{F(\eta)}{Q(\eta)} \frac{1}{\Omega^{\frac{1}{2}}(\eta)} d\eta$$

where  $k = 1$  corresponds to the potential for an ellipsoid. This can now be written explicitly in terms of  $x'_1, x'_2, x'_3$  and  $\tau$  as

$$\Omega_1 = C \int_{\tau}^{\infty} \left( 1 - \frac{x'_1}{a_1^2 + \eta} - \frac{x'_2}{a_2^2 + \eta} - \frac{x'_3}{a_3^2 + \eta} \right) \frac{d\eta}{[(a_1^2 + \eta)(a_2^2 + \eta)(a_3^2 + \eta)]^{\frac{1}{2}}} \quad (A10)$$

where functions of the form

$$\psi_i = x'_j x'_k \int_{\tau}^{\infty} \frac{d\eta}{(a_j^2 + \eta)(a_k^2 + \eta)[(a_1^2 + \eta)(a_2^2 + \eta)(a_3^2 + \eta)]^{\frac{1}{2}}} \quad (A11)$$

also satisfy equation (A9).

Jeffrey (loc. cit.) assumes that the velocity throughout the flow field can now be obtained as a function of the first and second derivatives of  $\Omega_1$  and  $\psi_1$  of the form:

$$\begin{aligned} u'_i = & U'_i + \frac{\partial}{\partial x'_i} (R\psi_1 + S\psi_j + T\psi_k) + W \frac{\partial \psi_k}{\partial x'_j} - V \frac{\partial \psi_j}{\partial x'_k} \\ & + A \left( x'_i \frac{\partial^2 \Omega_1}{\partial x'^2_i} - \frac{\partial \Omega_1}{\partial x'_i} \right) + H \left( x'_i \frac{\partial^2 \Omega_1}{\partial x'_i \partial x'_j} - \frac{\partial \Omega_1}{\partial x'_j} \right) \\ & + G' \left( x'_i \frac{\partial^2 \Omega_1}{\partial x'_i \partial x'_k} - \frac{\partial \Omega_1}{\partial x'_k} \right) + x'_j \left( H' \frac{\partial^2 \Omega_1}{\partial x'^2_i} + B \frac{\partial^2 \Omega_1}{\partial x'_i \partial x'_j} + F \frac{\partial^2 \Omega_1}{\partial x'_i \partial x'_k} \right) \\ & + x'_k \left( G \frac{\partial^2 \Omega_1}{\partial x'^2_i} + F' \frac{\partial^2 \Omega_1}{\partial x'_i \partial x'_j} + C \frac{\partial^2 \Omega_1}{\partial x'_i \partial x'_k} \right) \end{aligned} \quad (A12)$$

where  $A, B, C, F, F', G, G', H, H', R, S, T, U, V, W$  are constant, and  $U'_i$  is obtained from equation (A1), changed to primed coordinates.

Since the  $x'_i$ 's are now the independent coordinates, all derivatives of the type  $\partial x'_i / \partial x'_j$  are zero, and the system of equations (A12)

is found to satisfy the equation of continuity.

Substituting the assumed values of  $u_i'$  into equation (A4), it is found that the pressure must be given by

$$p = p_0 + 2 \left( A \frac{\partial^2 \Omega_1}{\partial x_1'^2} + B \frac{\partial^2 \Omega_1}{\partial x_2'^2} + C \frac{\partial^2 \Omega_1}{\partial x_3'^2} \right) + (F + F') \frac{\partial^2 \Omega_1}{\partial x_2' \partial x_3'} \\ + (G + G') \frac{\partial^2 \Omega_1}{\partial x_3' \partial x_1'} + (H + H') \frac{\partial^2 \Omega_1}{\partial x_1' \partial x_2'}$$

where  $p_0$  is the constant mean pressure at a distance from the ellipsoid. It should be noted that the expression found for the pressure does satisfy Laplace's equation, as required for flows of this type.

Substituting  $\Omega_1$  and  $\psi_i$  and their derivatives into equation (A12), setting  $\tau = 0$ , comparing term by term with equation (A5) and equating coefficients, 15 linear equations are obtained which uniquely determine the 15 coefficients.

Finally, substituting the values found for these coefficients into equation (A12), the velocity in the fluid in the vicinity of the particle is determined at all points.

To determine how these velocities act on the particle, the stresses in the fluid must be found. These stresses, for an incompressible fluid, are given by relations of the form:

$$\sigma_{x_i' x_i'} = -p + 2\mu \frac{\partial u_i'}{\partial x_i'} \quad , \\ \sigma_{x_i' x_j'} = \mu \left( \frac{\partial u_k'}{\partial x_j'} + \frac{\partial u_j'}{\partial x_k'} \right) \quad . \quad (A13)$$

To evaluate now the forces acting on the particle, the appropriate values from equation (A12) are substituted into equation (A13),  $\tau$  is set

equal to zero in order to obtain the forces at the surface of the particle, and equation (A13) is multiplied by the element of area on the surface of the ellipsoid, which has direction  $\underline{n}'$  given by the relation:

$$\underline{n}' = \frac{\nabla F}{|\nabla F|} = \frac{x'_1}{a_1} \underline{i}' + \frac{x'_2}{a_2} \underline{j}' + \frac{x'_3}{a_3} \underline{k}' . \quad (\text{A14})$$

The force  $\underline{df}$  acting on an element of area oriented perpendicularly to the  $x'_i$  coordinates is of the form:

$$\underline{df}_i = \left( \sigma_{x'_i c'_i} \underline{i}' + \sigma_{x'_k x'_i} \underline{j}' + \sigma_{x'_j x'_i} \underline{k}' \right) dS' .$$

The forces acting on the element of area  $\underline{n}' dS'$  on the surface of the ellipsoid are then given by

$$Y_i dS' = \underline{df}_i \cdot \underline{n}' = \left( \sigma_{x'_i x'_1} \frac{x'_1}{a_1} + \sigma_{x'_i x'_2} \frac{x'_2}{a_2} + \sigma_{x'_i x'_3} \frac{x'_3}{a_3} \right) dS' . \quad (\text{A15})$$

Carrying out the appropriate substitutions, the following expressions are obtained:

$$\begin{aligned} Y_1 &= -p_0 P \frac{x'_1}{a_1} + \frac{8P}{a_1 a_2 a_3} \left( A \frac{x'_1}{a_1} + H \frac{x'_2}{a_2} + G' \frac{x'_3}{a_3} \right) - K_0 \frac{x'_1}{a_1} \\ Y_2 &= -p_0 P \frac{x'_2}{a_2} + \frac{8P}{a_1 a_2 a_3} \left( H' \frac{x'_1}{a_1} + B \frac{x'_2}{a_2} + F \frac{x'_3}{a_3} \right) - K_0 \frac{x'_2}{a_2} \\ Y_3 &= -p_0 P \frac{x'_3}{a_3} + \frac{8P}{a_1 a_2 a_3} \left( G \frac{x'_1}{a_1} + F' \frac{x'_2}{a_2} + C \frac{x'_3}{a_3} \right) - K_0 \frac{x'_3}{a_3} \end{aligned} \quad (\text{A16})$$

where  $K_0$  is a constant of no consequence for this development, and  $P$  is given by

$$\frac{1}{P^2} = \prod_i^3 \frac{x_i'^2}{(a_i'^2 + \tau)^2} .$$

Carrying out the integration of equations (A15) over the surface of the ellipsoid, it is found that the result is zero; thus, no forces act on the particle, and this assumes the translational velocity of the fluid surrounding it.

Denoting by  $L_i$  the couple with axes  $x'_i$  acting on the particle, these can be obtained from expressions of the form

$$L_i = \int_S (x'_j Y'_k - x'_k Y'_j) ds' ,$$

where, upon substituting the terms from equations (A16) and integrating, it follows that:

$$L_1 = \frac{32}{3} (F' - F) ; L_2 = \frac{32}{3} (G' - G) ; L_3 = \frac{32}{3} (H' - H) , \quad (A17)$$

and substituting the values of  $F, F', G, G', H, H'$  :

$$\begin{aligned} L_1 &= K_1 (a_2^2 - a_3^2) e_{23} + (a_2^2 + a_3^2) (r_{23} - w'_1) \\ L_2 &= K_2 (a_2^2 - a_1^2) e_{13} + (a_3^2 + a_1^2) (r_{13} - w'_2) \\ L_3 &= K_3 (a_1^2 - a_2^2) e_{12} + (a_1^2 + a_2^2) (r_{12} - w'_3) \end{aligned} \quad (A18)$$

where again,  $K_1, K_2, K_3$  represent constants composed of coefficients that have been factored, and whose value is not needed for this development.

Since the particle is only subjected to the forces exerted by the fluid on its surface, all the resultant couples must vanish, and from equations (A18) it follows that

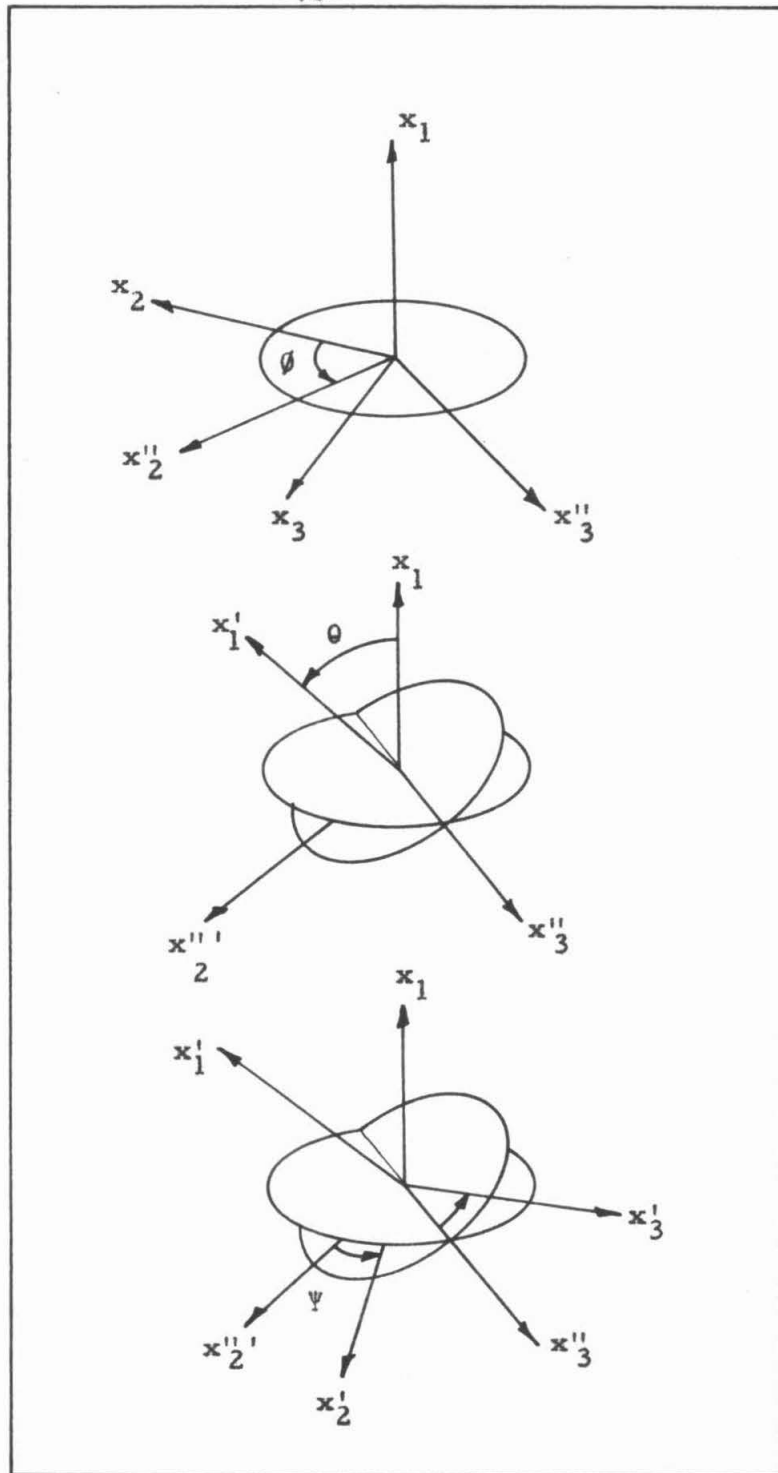


Figure 25. Transformation of the primed system of coordinates into the unprimed system by successive rotations.

$$\begin{aligned}
 (a_2^2 + a_3^2)\omega_1 &= a_2^2(r_{23} + e_{23}) + a_3^2(r_{23} - e_{23}) \\
 (a_3^2 + a_1^2)\omega_2 &= a_3^2(r_{13} + e_{13}) + a_1^2(r_{13} - e_{13}) \\
 (a_1^2 + a_2^2)\omega_3 &= a_1^2(r_{12} + e_{12}) + a_2^2(r_{12} - e_{12})
 \end{aligned}
 \tag{A19}$$

Equations (A19) represent the motion of the particle in the undisturbed fluid given by equation (A1). They can be solved exactly for the case of one-dimensional laminar motion, such as given by:

$$u_1 = u_2 = 0 \quad ; \quad u_3 = Gx_2 . \tag{A20}$$

To obtain the angular velocities of the particles, it is convenient to relate the coordinates  $x_1', x_2', x_3'$  fixed to the axes of the particle, to the coordinates  $x_1, x_2, x_3$  moving with the fluid but fixed in direction.

The relation between both systems is given by the Eulerian angles  $\theta$ ,  $\phi$ ,  $\psi$ , which represent a set of rotations of the unprimed system, that yields the primed system.

These rotations are [see Figure 25]: 1) counterclockwise rotation of the  $x_1, x_2, x_3$  system about the  $x_1$  axis by an angle  $\phi$  to yield the  $x_1, x_2'', x_3''$  system; 2) counterclockwise rotation of the  $x_1, x_2'', x_3''$  system about the  $x_3''$  axis by an angle  $\theta$  to yield the  $x_1', x_2''', x_3''$  system; 3) counterclockwise rotation of the  $x_1', x_2''', x_3''$  system about the  $x_1'$  axis by an angle  $\psi$  to yield the  $x_1', x_2', x_3'$  system. These rotations can be represented by the following matrix relations:

$$\begin{Bmatrix} x_1 \\ x_2' \\ x_3' \end{Bmatrix} = \begin{bmatrix} 1 & 0 & 0 \\ 0 & \cos\phi & \sin\phi \\ 0 & -\sin\phi & \cos\phi \end{bmatrix} \begin{Bmatrix} x_1 \\ x_2 \\ x_3 \end{Bmatrix} ; \quad \begin{Bmatrix} x_1' \\ x_2''' \\ x_3'' \end{Bmatrix} = \begin{bmatrix} \cos\theta & \sin\theta & 0 \\ \sin\theta & \cos\theta & 0 \\ 0 & 0 & 1 \end{bmatrix} \begin{Bmatrix} x_1 \\ x_2' \\ x_3'' \end{Bmatrix} ;$$

$$\begin{pmatrix} x'_1 \\ x'_2 \\ x'_3 \end{pmatrix} = \begin{bmatrix} 1 & 0 & 0 \\ 0 & \cos\psi & \sin\psi \\ 0 & -\sin\psi & \cos\psi \end{bmatrix} \begin{pmatrix} x''_1 \\ x''_2 \\ x''_3 \end{pmatrix} \quad (\text{A21})$$

so that the transformation matrix between the primes and unprimed system is given by:

$$\begin{pmatrix} x'_1 \\ x'_2 \\ x'_3 \end{pmatrix} = \begin{bmatrix} \cos\theta & \sin\theta\cos\phi & \sin\phi\sin\theta \\ -\sin\theta\cos\psi & \cos\phi\cos\psi\cos\theta - \sin\psi\sin\phi & \sin\phi\cos\theta\cos\psi + \sin\psi\cos\phi \\ \sin\theta\sin\psi & -\sin\theta\cos\theta\cos\phi - \sin\phi\sin\psi & -\sin\phi\sin\psi\cos\theta + \cos\psi\cos\phi \end{bmatrix} \begin{pmatrix} x_1 \\ x_2 \\ x_3 \end{pmatrix} \quad (\text{A22})$$

where each of the elements represents the direction cosines of the transformation matrix  $l_{ij} = [L]$ , such that the direction cosines between any two axes of the two systems are given by the intersection of the respective row and column in the following configuration:

	$x_1$	$x_2$	$x_3$
$x'_1$	$l_{11}$	$l_{12}$	$l_{13}$
$x'_2$	$l_{21}$	$l_{22}$	$l_{23}$
$x'_3$	$l_{31}$	$l_{32}$	$l_{33}$

(A23)

and the transformation is given by

$$\underline{x}' = [L]\underline{x} .$$

The flow, as it appears to the observer, is described by (A20) in the unprimed coordinate system, while the solution given by equations (A19) results from finding the potential of the ellipsoid with respect to the primed coordinates; therefore, to continue with the solution, equations (A20) must be expressed in the primed coordinate system in terms of the coefficients of the matrix  $[A]$ .

To do this, both  $\underline{u}$  and  $\underline{x}$  are transformed to the unprimed system of coordinates by the equation

$$\underline{u} = [L]^{-1}[A][L]\underline{x} . \quad (\text{A24})$$

and equating term by term with the coefficients of the flow characterized by equations (A20), the following matrix equation results:

$$[L]^{-1}[A][L] = \begin{bmatrix} 0 & 0 & 0 \\ 0 & 0 & 0 \\ 0 & G & 0 \end{bmatrix} \quad (\text{A25})$$

To solve the above system of equations, use is made of the fact that in the matrix  $[L]$ , the following relation exists between elements:

$$\sum_i l_{ik} l_{kj} = \delta_{kj} . \quad (\text{A26})$$

Computing the left-hand side term in equation (A25) corresponding to the non-zero term in the right hand side, the expression

$$l_{13}(a_{11}l_{12} + a_{12}l_{22} + a_{13}l_{32}) + l_{23}(a_{21}l_{12} + a_{22}l_{22} + a_{23}l_{32}) \\ + l_{33}(a_{31}l_{12} + a_{32}l_{22} + a_{33}l_{32}) = G$$

follows. Making use of the relationship given by equation (A26), it is found that the  $a_{ij}$ 's must be in the second order of the direction cosines, so that each bracket above can be set equal to  $G$  :

$$l_{13}(l_{13}G) + l_{23}(l_{23}G) + l_{33}(l_{33}G) = G$$

where this expression uniquely determines the  $a_{ij}$ 's to be

$$a_{ij} = G l_{13} l_{j2} . \quad (\text{A27})$$

which also satisfies the rest of the equations in the system.

Finally, the spins  $\omega_i^1$  of the  $x_i^1$  axes must be expressed in terms of the Eulerian angles, where the appropriate expression can be

found directly from Figure 23 to be

$$\begin{aligned}\omega_1^i &= \dot{\phi} \cos \theta + \dot{\psi} \\ \omega_2^i &= \dot{\theta} \sin \theta - \dot{\phi} \sin \theta \cos \psi \\ \omega_3^i &= \dot{\theta} \cos \theta + \dot{\phi} \sin \theta \sin \psi\end{aligned}\tag{A28}$$

The magnitude of the direction cosines is now found by comparing table (A23) and matrix (A22) and then evaluating the  $a_{ij}$ 's. Finally, substituting the values of the  $a_{ij}$ 's and the  $\omega_i^i$ 's into equations (A19), the motion of a rotationally symmetric ellipsoid ( $a_2 = a_3$ ) is found to be given by:

$$\dot{\theta} = \frac{1}{2}Gp \sin \theta \cos \theta \sin 2\phi\tag{A29}$$

$$\dot{\phi} = \frac{1}{2}G(1 + p \cos 2\phi)\tag{A30}$$

where

$$p = a_1^2 - a_2^2 / a_1^2 + a_2^2.\tag{A31}$$

The motions of interest are given by  $\dot{\theta}$  and  $\dot{\phi}$ . The  $\dot{\psi}$  rotation represents the spin of the particle about its own axis of revolution and is of no interest for the present development.

The result is that each particle is subjected to hydrodynamic effects which result in the motion described by equations (A29) and (A30). Defining  $F(\theta, \phi)$  as the fraction of particles with orientation  $\theta, \phi$ , a transport flux density  $\underline{i}_{str}$  can be defined as the motion of the end of the semiaxis of the particle on the unit sphere centered at the center of the particle. In spherical coordinates, this flux is given by

$$\underline{i}_{str} = F(\theta, \phi)(\dot{\theta}\underline{e}_\theta + \dot{\phi} \sin \theta \underline{e}_\phi)\tag{A32}$$

where  $\underline{e}_\theta$  and  $\underline{e}_\phi$  are the usual unit vectors of the spherical system of coordinates.

A. 2 Motion of the Particles Due to Brownian Motion and Rotary Diffusion.

In a state of equilibrium, in the absence of external forces, the concentration of a molecular species is uniform throughout a single phase. If the concentration is not uniform, the molecules will tend to move from regions of higher to lower concentration, as a consequence of the Second Law of Thermodynamics, which indicates that the entropy of the system will be a maximum when the molecules are distributed with statistical uniformity throughout the system.

Given a difference of concentration, a flow will ensue as a result of the thermal energy of the molecules, i. e., due to their Brownian motion. The speed at which a given molecule diffuses is characterized by its diffusion constant, which is a function of the shape, size, and mass of the molecule, as well as the temperature and viscosity of the medium.

Brownian motion also influences the orientation of molecules when these exhibit a preferential orientation. In particular, in a system of particles of ellipsoidal shape suspended in a medium where, as in the case under consideration, an external (hydrodynamic) influence tends to produce preferential orientations and this influence is suddenly removed, the orientation will gradually disappear until the distribution of orientation is again completely random. The speed at which complete randomness is achieved from a given distribution of orientation is characterized by the rotational diffusion constant.

Letting  $i_{diff}$  be the flux density of orientation of a population of molecules in which a distribution of orientation  $F(\theta, \phi)$  exists, then the flux density is related to  $F$  by the following equation:

$$\underline{i}_{\text{diff}} = -D \nabla F(\theta, \phi) \quad (\text{A33})$$

where  $\nabla$  is the gradient operator in spherical coordinates without  $r$  dependence. This equation defines  $D$ , the rotational diffusion constant.

Ferrin<sup>(20)</sup> has found the following explicit expression for the rotary diffusion constant for ellipsoids of revolution

$$D = \frac{3kT}{16\pi\eta_m a_1^3} \left( -1 + 2 \ln \frac{2a_1}{a_2} \right) = \frac{D_p}{\eta_m} \quad (\text{A34})$$

where  $k$  is Boltzmann's constant,  $T$  is the absolute temperature, and  $\eta_m$  is the viscosity of the medium. The last equality is shown for future reference to illustrate the form of dependence of the diffusion constant on the viscosity.

### A. 3 Distribution Function.

The distribution function which yields the angular concentration of the main axis of the particle is calculated by considering the competition of the hydrodynamic forces on the particle, which produces a flux transport  $\underline{i}_{\text{str}}$  given by equation (A32), and the flux due to Brownian motion given by equation (A33) which tries to diminish any unevenness in the distribution of orientations. For the steady state, the following relation must hold:

$$\nabla \cdot (\underline{i}_{\text{str}} + \underline{i}_{\text{diff}}) = 0. \quad (\text{A35})$$

Substituting for  $\dot{\theta}$  and  $\dot{\phi}$  the values of the equations of motion given by equations (A29) and (A30) and evaluating equation (A35), the following expression results:

$$\nabla^2 F(\theta, \phi) - \frac{G}{2D} [1 + \phi \cos 2\phi] \frac{\partial F}{\partial \phi} + \phi \sin \theta \cos \theta \sin 2\phi \frac{\partial F}{\partial \theta} - 3\phi \sin^2 \theta \sin 2\phi F] = 0 \quad (A36)$$

For  $p \leq 1$ , the solution of (A36) is obtained as a series of spherical harmonics of the form

$$F(\theta, \phi) = \sum_{h=0}^{\infty} p^h F_h(\theta, \phi) \quad (A37)$$

where

$$F_h = \frac{1}{2} \sum_{n=0}^h a_{no, h} P_{2n} + \sum_{n=1}^h \sum_{m=1}^n (a_{mn, h} \cos 2m\phi + b_{nm, h} \sin 2m\phi) P_{2n}^{2m} \quad (A38)$$

in which

$P_{2n}$  = spherical harmonics of the second order of  $\cos \theta$ ,

$P_{2n}^{2m}$  = associated Legendre functions =  $\sin^{2m} \theta \frac{d^{2m} P_{2n}}{(d \cos \theta)^{2m}}$ .

The constants  $a_{nm, h}$  are determined by substituting the series (A37) into equation (A36) and equating terms with the same argument. It is found that all constants of this group can be expressed in terms of  $a_{00, 0}$ , and that constants of the type  $a_{no, h}$  are all zero except for  $a_{00, 0}$ . Finally, to evaluate  $a_{00, 0}$ ,  $F(\theta, \phi)$  is normalized by setting the integral of  $F(\theta, \phi)$  over the surface of the unit sphere equal to unity. Thus

$$\int_0^{2\pi} \int_0^{\pi} F(\theta, \phi) \sin \theta \, d\theta \, d\phi = 1.$$

Because of the orthogonality, all terms of  $F(\theta, \phi)$  vanish except for  $F_0$ , which, upon integration, yields

$$a_{00, 0} = \frac{1}{4\pi}.$$

The final result is

$$F = \frac{1}{4\pi} \left[ 1 + p \left( -\frac{1}{2} \cos 2\phi + \frac{3}{\sigma} \sin 2\phi \right) \frac{3 \sin^2 \theta}{1 + \frac{36}{\sigma^2}} + \dots \right] \quad (\text{A39})$$

where  $\sigma = G/D$ ; for small values of  $\sigma$ , i. e., large influence of Brownian motion, and small gradients, this reduces to

$$F = \frac{1}{4\pi} \left[ 1 + \frac{\sigma\phi}{4} \sin 2\phi \sin^2 \theta + \dots \right] . \quad (\text{A40})$$

#### A. 4 Optical Behavior.

The optical characteristics of the system are determined by the orientation of ellipsoidal particles of permittivity  $\epsilon$  suspended in a medium of permittivity  $\epsilon_m$ .

The particles under consideration are assumed to be considerably smaller than the wavelength of light, so that at any given instant the electromagnetic field felt by the particle can be regarded as essentially uniform throughout the particle. This assumption permits us to study the characteristics of the composite medium in the steady state, and the analysis is based on finding how a distribution of ellipsoids of permittivity  $\epsilon$  in a suspending medium of permittivity  $\epsilon_m$  affects a uniform electric field applied to this system.

The effect of the medium on the electric field is then set to be identical to the effect of the medium on the  $\underline{E}$  vector of a beam of light. Furthermore, both the particle and the suspending medium are assumed to be non-magnetic, and their permeabilities are taken as the one of free space, so that the analysis of the electric component of the beam of light suffices to describe the phenomenon in its entirety.

A uniform electric field  $\underline{E}$  applied to a particle suspended in

a medium will induce a polarization  $\underline{P}$ , which is a result of the polarization  $\underline{P}_m$  of the medium, and  $\underline{P}_p$  of the particle, where

$$4\pi\underline{P}_m = (\epsilon_m - 1)\underline{E} \quad (\text{A41})$$

and

$$\underline{P} = \underline{P}_m + \underline{P}_p \quad (\text{A42})$$

The particle is characterized by its polarizabilities  $\alpha_i'$  and permittivities  $\epsilon_i'$ , along with the  $x_i'$  coordinates fixed to the particle and already used to describe its hydrodynamic behavior.

$\underline{P}_p$  is found by determining first the electric field  $\underline{E}'_{-p_i}$  within the particles. This electric field  $\underline{E}'_{-p_i}$  is a result of the electric field external to the particle  $\underline{E}'_i$  plus the polarization  $\underline{P}'_{-p_i}$  due to this field, modified by a shape factor  $L_i$  which accounts for the asymmetry of the internal field.

These shape factors reduce to simple expressions for the cases of a sphere, flat disc perpendicular to the field, and elongated cylinder parallel to the field. They represent the relative amount by which the shape of an object of dielectric  $\epsilon_1$ , in a medium of dielectric  $\epsilon_2$ , decreases the overall field strength due to the appearance of charges at the interface between the two media. They have been deduced analytically by Rayleigh<sup>(21)</sup>, and are included graphically in Figure 26.

The field along each of the axes of the particle is then given by:

$$\underline{E}'_{-p_i} = \underline{E}'_i + L_i \underline{P}'_{-p_i} \quad .$$

In view of the polarizability of the particle, the particle will then exhibit an electric moment  $m_i'$  :

$$\underline{m}'_i = \alpha_i \left( \underline{E}'_i + \frac{1}{\epsilon_i'} L_i \underline{P}'_{-p_i} \right) = \alpha_i (1 + L_i K_i) \underline{E}'_i = A_i \underline{E}'_i \quad (\text{A43})$$

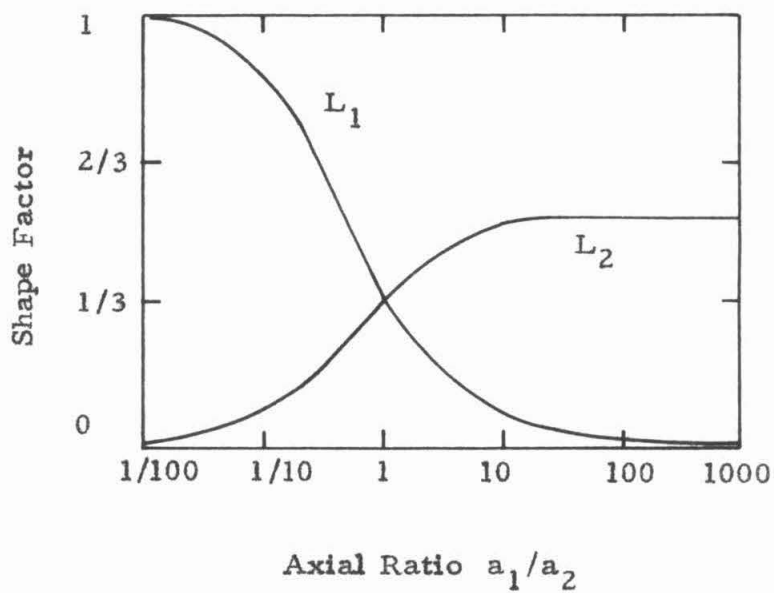


Figure 26. Shape factors  $L_1$  and  $L_2$  as a function of axial ratio.

In the coordinate axes  $x_i$  fixed in direction as in the hydrodynamic case, the electric moment becomes

$$m_j = \sum_i A_i E_i l_{ij} \quad (\text{A44})$$

where the  $l_{ij}$ 's are the cosines of the angles between the primed and unprimed systems of coordinates, given by the matrix (A22).

Furthermore, each  $\underline{E}_i'$  has components along the  $x_i$  system of coordinates such that

$$\underline{E}_i' = E_j l_{ij} ; \quad (\text{A45})$$

thus, the moments in the unprimed (fixed) system of coordinates, due to each electric component  $\underline{E}_j$  in this system, are given by

$$m_{kj} = \left( \sum_i A_i l_{ik} l_{ij} \right) E_j . \quad (\text{A46})$$

For an ellipsoid of revolution, whose axis of revolution is the  $x_1'$  axis,  $e_2' = e_3'$ ; thus,  $L_2 = L_3$  and  $A_2 = A_3$ , and the system (A46), making use of equation (A26), reduces to:

$$\begin{aligned} m_{11} &= [A_2 + (A_1 - A_2)] l_{11}^2 E_1 = B_{11} E_1 \\ m_{21} &= (A_1 - A_2) l_{11} l_{12} E_1 = B_{21} E_1 \\ m_{31} &= (A_1 - A_2) l_{11} l_{13} E_1 = B_{31} E_1 \end{aligned} \quad (\text{A47})$$

Noting that  $B_{21} = B_{12}$ ,  $B_{23} = B_{32}$ , and  $B_{31} = B_{13}$ , the corresponding components of the moment in the  $x_2$  and  $x_3$  directions can be obtained from equations (A47) by cyclic permutation of the indices and subscripts.

$N_p$  particles per unit volume, oriented according to the distribution function given by equation (A39), where each particle contributes a component to the moment given by equation (A47), will produce

moments  $M_{kj}$  in a system of particles and suspending medium given by

$$M_{kj} = \frac{\int m_{kn} dN}{\int dN} = \int m_{kj} F d\Omega = P_{kj} E_j \quad (A48)$$

where  $d\Omega = \sin\theta d\theta d\phi$  and  $M_{kj}$  is now the moment per unit volume due to the field in the  $j$  direction, and the characteristics of the particle along the  $k$  direction, both directions being along the unprimed system of coordinates.

To compute the moments per unit volume by equation (A48), the cosines between the two systems of coordinates must be expressed in terms of the transformation given by the matrix (A22), where the  $\psi$  angle is set to zero, since the ellipsoid is rotationally symmetric about the  $x'_1$  axis; and along any position it would yield the same result, zero then being the most convenient one in terms of simplification of the expressions.

Carrying out the substitutions in equations (A47) and solving for  $P_{kj}$  yields

$$\begin{aligned} P_{11} &= \int_0^\pi \int_0^{2\pi} F [A_2 + (A_1 - A_2) \sin^2 \theta \sin^2 \phi] \sin \theta d\theta d\phi \\ P_{22} &= \int_0^\pi \int_0^{2\pi} F [A_2 + (A_1 - A_2) \sin^2 \theta \cos^2 \phi] \sin \theta d\theta d\phi \\ P_{23} &= (A_1 + A_2) \int_0^\pi \int_0^{2\pi} F \sin^3 \theta \sin 2\phi d\theta d\phi \end{aligned} \quad (A49)$$

$$P_{33} = \int_0^\pi \int_0^{2\pi} F[A_2 + (A_1 - A_2)\cos^2\theta] \sin\theta \, d\theta \, d\phi$$

The elements  $P_{kj}$  form a symmetric matrix where  $P_{kj} = P_{jk}$  and  $P_{12} = P_{13} = 0$ , because of the geometry of the flow, according to which the particles are randomly oriented with respect to the plane of flow. Since there is an equal number of particles above and below it, the moments cancel each other. The matrix thus reduces to

$$[P_{kj}] = \begin{bmatrix} P_{11} & 0 & 0 \\ 0 & P_{22} & P_{23} \\ 0 & P_{23} & P_{33} \end{bmatrix} \quad (A50)$$

To find the principal directions in the system, the matrix (A50) must be diagonalized, so that the magnitude of the angle through which the system is rotated about the  $x_1$  axis represents the location of the extinction angle  $\chi$  of the system. To rotate the matrix (A50), the following equation must be solved for  $\chi$ :

$$[\chi][P_{kj}][\chi]^{-1} = [P_{kj}^*]$$

where  $[P_{kj}^*]$  is the diagonalized form, and  $[\chi]$  is the rotation matrix:

$$[\chi] = \begin{bmatrix} 1 & 0 & 0 \\ 0 & \cos\chi & \sin\chi \\ 0 & \sin\chi & \cos\chi \end{bmatrix}$$

The result is

$$\tan 2\chi = \frac{2P_{23}}{P_{22} - P_{33}} \quad (A51)$$

where the elements along the diagonal are now given by

$$P_{11}^* = P_{11}$$

$$P_{22}^* = (P_{22} + P_{33}) + [(P_{22} - P_{33})^2 + 4p_{23}]^{\frac{1}{2}}$$

$$P_{33}^* = (P_{22} + P_{33}) - [(P_{22} - P_{33})^2 + 4p_{23}]^{\frac{1}{2}}$$

Substituting equation (A49) into equation (A51) yields the following expression:

$$\tan 2\chi = \frac{\int_0^\pi \int_0^{2\pi} F(p, \sigma, \theta, \phi) \sin^3 \theta \sin 2\phi \, d\theta \, d\phi}{\int_0^\pi \int_0^{2\pi} F(p, \sigma, \theta, \phi) \sin^3 \theta \cos 2\phi \, d\theta \, d\phi}$$

Using the series (A40) for  $F$ , for values of  $\sigma \leq 1.5$  and  $p \leq 1$ ,

Peterlin and Stuart (loc. cit.) find that

$$\chi(\sigma, p) = \frac{\pi}{4} - \frac{\sigma}{12} + \frac{\sigma^3}{1296} \left(1 + \frac{24p^2}{35}\right) + \dots \quad (A53)$$

To find the magnitude of the birefringence, i. e., the relative difference in index of refraction between the two principal directions, the differences in permittivities along the principal directions must be found.

The polarization  $\underline{P}_p$  in the suspending medium, due to the presence of  $N_p$  ellipsoidal particles, can now be found as

$$\underline{P}_p = [e_m] N_p \underline{M} \quad (A54)$$

and from equation (A48):

$$\underline{P}_p = [e_m] N_p [p] \underline{E} \quad (A55)$$

Substituting into equation (A42), one obtains

$$\underline{P} = \frac{1}{4\pi} ([e_m] - [I]) \underline{E} + [e_m] N_p [p] \underline{E} \quad (A56)$$

where  $[I]$  is the unitary matrix.

Letting  $[e]$  be the permittivity of the whole system, the matrix

equation (A56) can be written as

$$\underline{P} = \frac{1}{4\pi} ([\epsilon] - [I]) \underline{E} \quad (A57)$$

where

$$[\epsilon] = \begin{bmatrix} \epsilon_{11} & 0 & 0 \\ 0 & \epsilon_{22} & \epsilon_{23} \\ 0 & \epsilon_{23} & \epsilon_{33} \end{bmatrix}; [\epsilon_m] = \epsilon_m [I]; [I] = \begin{bmatrix} 1 & 0 & 0 \\ 0 & 1 & 0 \\ 0 & 0 & 1 \end{bmatrix}.$$

Equating expressions (A56) and (A57) yields

$$[\epsilon] - [\epsilon_m] = 4\pi [\epsilon_m] N_p [p]. \quad (A58)$$

Using now the diagonalized form of  $[p]$ , a new diagonal matrix results whose terms along the diagonal  $\epsilon_{11}$ ,  $\epsilon_{22}$ ,  $\epsilon_{33}$ , are the principal permittivities in the system. Equating term by term on both sides of equation (A58) yields

$$\epsilon_{22} - \epsilon_m = 4\pi \epsilon_m N_p p_{22}^*$$

$$\epsilon_{33} - \epsilon_m = 4\pi \epsilon_m N_p p_{33}^*.$$

The difference of permittivities that is observable in the chosen geometry is then obtained by subtracting one equation from the other; namely,

$$\epsilon_{22} - \epsilon_{33} = 4\pi \epsilon_m N_p (p_{22}^* - p_{33}^*). \quad (A59)$$

Under the quasi-stationary conditions under which these equations have been derived, the permittivities can be substituted for the squares of the indices of refraction such that

$$\epsilon_{22} - \epsilon_{33} = n_{22}^2 - n_{33}^2 = 2n(n_{22} - n_{33}),$$

where  $n$  is the refractive index of the system of particles and suspending medium, which can be taken as having the same values as the index of refraction of the latter. Substituting this last expression into

equation (A59) yields

$$n_{22} - n_{33} = 2\pi n N_p (p_{22}^* - p_{33}^*) .$$

Peterlin and Stuart (loc. cit.) find that the difference  $(p_{22}^* - p_{33}^*)$  can be separated into two parts; one,  $(g_{x_1'} - g_{x_2'})$ , is a function of the optical properties of the particle along its  $x_1'$  and  $x_2'$  axes and results from equation (A43); and the other,  $f(\sigma, p)$ , is related to the orientation of the particles, and thus their distribution function results from equation (A49), namely:

$$N(p_{22}^* - p_{33}^*) = V(g_{x_1'} - g_{x_2'})f(\sigma, p)$$

where  $V$  is the volume of the particle,

$$g_{x_1'} - g_{x_2'} = \frac{3\epsilon_m}{4\pi} \frac{\epsilon_m(\epsilon_1' - \epsilon_2') + (\epsilon_1' - \epsilon_m)(\epsilon_2' - \epsilon_m) \frac{1}{4\pi} (L_1 - L_2)}{[\epsilon_m + \frac{1}{4\pi} L_1(\epsilon_1' - \epsilon_m)][\epsilon_m + \frac{1}{4\pi} L_2(\epsilon_2' - \epsilon_m)]} .$$

and

$$f(\sigma, p) = \frac{\sigma p}{15} - \frac{\sigma^3 p}{1080} \left(1 + \frac{6p^2}{35}\right) + \dots$$

so that

$$\Delta n = \frac{2\pi N_p}{n} V(g_{x_1'} - g_{x_2'})f(\sigma, p) . \quad (A60)$$

For small values of  $\sigma$ ,  $f(\sigma, p) \simeq \sigma p / 15$ . The term  $N_p V$  which gives the total concentration in terms of volume of particles per total volume of the solution can be converted to weight concentration,  $c$ , per unit volume by multiplying and dividing equation (A59) by  $\rho_p$ , the particle density, to yield

$$\Delta n = \frac{2\pi p}{15\rho_p n D_p} (g_{x_1'} - g_{x_2'}) c G \eta_m . \quad (A61)$$

APPENDIX B

Sample Data

Date: January 9, 1963

Experiment No.: 10

Concentrations. TMV: 0.359%, SBMV:  $\pm$  0.123%, Other: in Versene

$\eta$	WINDOW $\alpha_2$
0 <sub>1</sub>	814
7	397
15	406
20	408
25	423
30	431
35	451
40	454
55	499
60	512
65	527
70	542
80	557
90	568
0 <sub>2</sub>	-
95	562
100	558
110	543
115	536
120	513
130	487
140	464
150	437
160	412
170	399
180	393
190	393
200	407
0 <sub>3</sub>	812
50	487

G	$\theta$ MILLIVOLT	REST NULL	STREAM NULL CW	$\chi_{CW}$	STREAM NULL CC	$\chi_{CC}$	REST NULL
1.31	.812	18.42	18.79	82.30	17.86	104.57	18.41
3.24	.814	18.42	19.46	87.56	17.18	100.12	18.40
5.18		18.41	20.14	90.17	16.48	98.18	18.42
9.33	.818	18.42	21.54	91.02	15.09	97.32	18.42
14.0		18.42	23.08	91.16	13.51	97.19	18.42
21.9	.812	18.42	25.64	91.15	10.95	97.21	18.42
26.0		18.41	26.59	91.12	9.65	97.25	18.42
31.1	.814	18.42	28.65	81.03	7.95	97.34	18.42

All rest null at  $\chi = 7^\circ$

Data Reduction

Date: February 18, 1963

Experiment No. : 10

Concentrations. TMV: .359<sup>o</sup>/. SBMV: .123<sup>o</sup>/.

Window Correction.  $\delta_w$ : 0.0858. Isocline: 55<sup>o</sup>.62

G	DATA				ZERO CORRECTION				WINDOW CORRECTION			
	$\delta'_e$		$\chi_e$		$\delta_e$		$\chi_e$		$\delta$		$\chi$	
	CW	CC	CW	CC	CW	CC	CW	CC	CW	CC	CW	CC
1.31	0.37	0.55	82.50	104.95	0.45	0.45	88.99	100.59	0.45	0.43	94.43	95.16
3.24	1.04	1.22	87.93	100.20	1.12	1.12	90.21	98.35	1.12	1.10	92.40	96.19
5.18	1.73	1.94	90.28	98.30	1.81	1.85	91.65	97.07	1.81	1.83	93.00	95.76
9.33	3.12	3.33	91.03	97.53	3.20	3.24	91.79	96.81	3.20	3.22	92.56	96.06
14.0	4.66	4.91	91.27	97.32	4.74	4.82	91.78	96.83	4.74	4.80	92.30	96.33
21.9	6.76	7.48	91.25	97.35	7.34	7.39	91.57	97.03	7.34	7.37	91.90	96.70
26.0	8.18	8.78	91.20	97.42	8.26	8.69	91.49	97.17	8.26	8.67	91.79	96.88
31.1	10.23	10.48	91.05	97.57	10.31	10.39	91.28	97.35	10.31	10.37	91.51	97.12

Note on Data Reduction

The data of the window is obtained as outlined in Section 3.3. A calibrated dial permits interpolation of the readings of the verniers to  $0.001^\circ$ , and by computer the best sinusoid that fits the experimental points is obtained. This yields the amount of birefringence and the corresponding position of the isocline of the windows.

$\theta_1$ ,  $\theta_2$ , and  $\theta_3$  are temperature readings from a thermocouple located in the Couette cell, in millivolts. CW and CC refer to clockwise and counterclockwise rotation.

The zero correction refers to the correction necessary to account for the error in quadrature. The window correction refers to the one given by equations (17) and (18).

The Couette cell used has a 0.2 cm gap between cylinders, and a 5 cm path length in the gap. For the  $5460 \text{ \AA}$  wavelength, the amount of retardation per unit length, in  $\text{\AA}/\text{cm}$ , can then be obtained by multiplying the amount of observed optical rotation by 6.06.

REFERENCES

1. Maxwell, J. C., "On Double Refraction in a Viscous Fluid in Motion," Proc. Roy. Soc. A22, 46 (1873).
2. Peterlin, A. and Stuart, H. A., Hand- und Jahrbuch der chemischen Physik, Bd. VIII, Abt. 1B, "Doppelbrechung, insbesondere künstliche Doppelbrechung," Becker and Erler, Leipzig, (1943).
3. Wayland, J. H., "Mesures photoelectriques en birefringence d'ecoulement," Comptes Rendus, 249, 1228 (1959).
4. Born, M. and Wolf, E., Principles of Optics, Pergamon Press (1959).
5. Walker, M. J., "Matrix Calculus and the Stokes Parameters of Polarized Radiation," Am. J. Phys., 22, 170 (1954).
6. Shurcliff, W. A., Polarized Light, Harvard University Press (1962).
7. Wayland, J. H. and Badoz, J., "Determination photoelectrique de la position des lignes neutres d'un milieu faiblement birefringent," Comptes Rendus, 250, 688 (1960).
8. Sutura, S. P., "Streaming Birefringence as a Hydrodynamic Research Tool," Doctoral Thesis, California Institute of Technology (1960).
9. Leray, J., "Sur la verification de la theorie de l'orientation des particules rigides par birefringence d'ecoulement," Journal de Chimie Physique, 316 (1961).
10. Hearst, J. H. and Vinograd, J., "The effect of angular velocity on the sedimentation behavior of deoxyribonucleic acid and tobacco mosaic virus," Archives of Biochemistry and Biophysics, Vol. 92, No. 2, 206 (1961).
11. Edsal, J. T., Rich, A., and Goldstein, M., "An instrument for the study of double refraction of flow at low and intermediate velocity gradients," Rev. Sci. Instr., 23, 695 (1952).
12. Zimm, B. H., "Photoelectric Flow Birefringence Instrument of High Sensitivity," Rev. Sci. Instr., 9, 360 (1958).
13. Collins, D. J. and Wayland, J. H., "Hydrodynamic Interactions of Submicroscopic Particles, I. Viscometric Studies," Journal of the Rheological Society (in press).

14. Konrad, M., "A Preparation of Southern Bean Mosaic Virus," private communication.
15. Einstein, A., The Theory of the Brownian Movement, Dover Publications (1956).
16. Boedtker, H. and Simmons, N. S., "The Preparation and Characterization of Essentially Uniform Tobacco Mosaic Virus," J. Am. Chem. Soc., 10, 2550 (1958).
17. Miller, G. L. and Price, W. C., "Physical and Chemical Studies of Southern Bean Mosaic Virus. I. Size, Shape, Hydration, and Elementary Composition," Archives of Biochemistry and Biology, Vol. 10 (1946).
18. Jeffrey, G. B., "The Motion of Ellipsoidal Particles Immersed in a Viscous Fluid," Proc. Roy. Soc. (London), A102, 161 (1922).
19. Bateman, H., Partial Differential Equations of Mathematical Physics, Chapter 8, "Ellipsoidal Coordinates," Cambridge University Press, London (1932).
20. Perrin, F., "Mouvement Brownien d'un Ellipsoïde, (I.) Dispersion Dielectrique pour des Molecules Ellipsoïdales," J. Phys. Radium, 5, Series 7, 497 (1934).
21. Rayleigh, Lord, "On the Incidence of Aerial Waves upon Small Obstacles in the Form of Ellipsoids or Elliptic Cylinders, and on the Passage of Electric Waves through a Circular Aperture in a Conducting Screen," Phil. Mag., 44, 28 (1897).